RF Project 761050/711050
Progress Report

the ohio state university
research foundation
1314 kinnear road
columbus, ohio
43212

IGNITION, COMBUSTION, DETONATION, AND QUENCHING OF REACTIVE MIXTURES

H00 015

Rudolph Edse
Department of Aeronautical and Astronautical Engineering

For the Period
April 1, 1978 - March 31, 1979

U.S. DEPARTMENT OF THE AIR FORCE
Air Force Office of Scientific Research
Bolling Air Force Base
Washington, D.C. 20332

Grant No. AFOSR-78-3604

November, 1979

UNCLASSIFIED

SECURITY CLASSIFICATION OF THIS PAGE (When Data Entered)

REPORT DOCUMENTATION PAGE

READ INSTRUCTIONS BEFORE COMPLETING FORM

1. REPORT NUMBER: AFOSR-TR-80-0302	2. GOVT ACCESSION NO.: AD-A083737
3. RECIPIENT'S CATALOG NUMBER	
4. TITLE (and Subtitle): Ignition, Combustion, Detonation, and Quenching of Reactive Mixtures.	5. TYPE OF REPORT & PERIOD COVERED: INTERIM rept. 1 Apr 78 — 31 Mar 79
	6. PERFORMING ORG. REPORT NUMBER
7. AUTHOR(s): RUDOLPH EDSE	8. CONTRACT OR GRANT NUMBER(s): AFOSR-78-3604
9. PERFORMING ORGANIZATION NAME AND ADDRESS: THE OHIO STATE UNIVERSITY RESEARCH FOUNDATION, 1314 KINNEAR ROAD COLUMBUS, OHIO 43212	10. PROGRAM ELEMENT, PROJECT, TASK AREA & WORK UNIT NUMBERS: 2308 A2 61102F
11. CONTROLLING OFFICE NAME AND ADDRESS: AIR FORCE OFFICE OF SCIENTIFIC RESEARCH/NA BUILDING 410 BOLLING AFB, DC 20332	12. REPORT DATE: NOV 79
	13. NUMBER OF PAGES: 51
14. MONITORING AGENCY NAME & ADDRESS (if different from Controlling Office)	15. SECURITY CLASS. (of this report): UNCLASSIFIED
	15a. DECLASSIFICATION/DOWNGRADING SCHEDULE

16. DISTRIBUTION STATEMENT (of this Report)

Approved for public release; distribution unlimited.

17. DISTRIBUTION STATEMENT (of the abstract entered in Block 20, if different from Report)

18. SUPPLEMENTARY NOTES

19. KEY WORDS (Continue on reverse side if necessary and identify by block number)

DETONATION INDUCTION DISTANCE
FLAME AND DETONATION QUENCHING
FLAME SPEED
DEFLAGRATION,
FLASH-BACK
QUENCHING DISTANCE
INHIBITOR
NORMAL OBLIQUE SHOCK WAVE
RAMJET

400 015

20. ABSTRACT (Continue on reverse side if necessary and identify by block number)

The effects of initial gas temperature, pressure, density, and energy transfer to the gas in the detonation wave have been studied to develop an equation which can be used to predict the length of transition from deflagration to detonation (induction distance) in confined and unconfined combustible gas mixtures. Flame speeds of various hydrogen-oxygen-inert gas mixtures have been measured to determine the relationship between flame speed (deflagration) and induction distance. A nozzle burner having a sine curve contour was used for these experiments to obtain well-defined laminar flame cones permitting reliable and

DD FORM 1 JAN 73 1473 EDITION OF 1 NOV 65 IS OBSOLETE

UNCLASSIFIED

reproducible evaluations. The quenching distances of methane-air, methane-oxygen, acetylene-air, and hydrogen-air flames were not affected by potassium chloride, sodium-bicarbonate, or potassium phosphate coatings on the quenching surfaces. It was also found that the quenching distances of these flames are independent of the linear speed of the unburned gas as long as the flows are laminar. Variations of the burner width also did not affect the quenching distances. However, rather significant increases of the quenching distances were observed when the narrow sides between the quenching surfaces were closed. New iteration formulas have been developed to simplify and reduce the computational work for calculating detonation parameters and the performance of thermal engines (ramjet, rocket, gas turbine, and internal combustion engine).

TABLE OF CONTENTS

LIST OF TABLES

LIST OF FIGURES

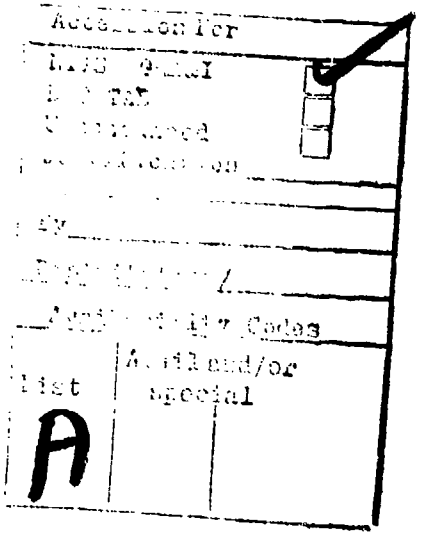

LIST OF SYMBOLS

A	Area of duct
$a^{(j)}(T)$	Coefficient of equilibrium constant $K_p^{(j)}$ of chemical change (j) at temperature T
c_s^T	Entropy coefficient of a gas or gas mixture at temperature T
e^T	Absolute internal energy of a unit mass of any substance at temperature T
$E_{o,i}$	Absolute internal energy of one mole of species i at T = OK
f	Fuel to air mass ratio $\left(f = \frac{\dot{m}_{FUEL}}{\dot{m}_{air}}\right)$
$\left(\frac{H-E_o}{\mathcal{R}T}\right)_i^T$	Reduced sensible enthalpy of species i at temperature T
h^T	Absolute enthalpy of a unit mass of any substance at temperature T
$\left(\frac{H_f}{\mathcal{R}T}\right)_i^T$	Reduced formation enthalpy of species i at temperature T
$K^{(j)}$	Equilibrium constant of chemical change (j) in terms of mole fractions $\left(K^{(j)} = K_p^{(j)} \cdot p^{-\Delta\nu^{(j)}}\right)$
$\mathcal{m}$	Molecular mass
$\dot{m}$	Mass flow rate
p	Static pressure
$\mathcal{R}$	Universal gas constant $\left(8314.33 \frac{J}{kmol\ K}\right)$
$R = \frac{\mathcal{R}}{\mathcal{m}}$	Specific gas constant

LIST OF SYMBOLS (Continued)

$\left[\left(\frac{S^{p=1}}{\mathcal{R}}\right)\Big/\frac{\partial}{\partial n}_T\right]_i^T \equiv c_s^T$	Entropy coefficient of species i at temperature T
T	Absolute temperature
u	Gas speed (relative to laboratory)
v	Specific volume
w	Wave speed (relative to gas)
$\gamma = \frac{c_p}{c_v}$	Ratio of normal specific heats (= isentropic coefficient)
$\gamma_{eff} = \frac{c_{p_{eff}}}{c_{v_{eff}}}$	Ratio of specific heats of chemically reacting gas mixture (= isentropic coefficient)
$\nu_i^{(\ell)}$	Number of moles of species i participating in chemical change (ℓ) = stoichiometric mole numbers (positive for products and negative for reactants)
$\nu_{e\ell}^{(i)}$	Moles of element type $e\ell$ in species i
$\rho = \frac{1}{v}$	Density
η_i	Mole fraction of species i in mixture of gases
$\Delta\nu^{(\ell)} \equiv \sum\nu_i^{(\ell)}$	Change of mole numbers of chemical change (ℓ)

Subscripts and Superscripts

DE	Diffuser exit
Dt	Diffuser throat
NE	Nozzle exit
Nt	Nozzle throat

LIST OF SYMBOLS (Continued)

Subscripts and Superscripts (Continued)

i	Inlet or species
c	Combustion chamber
o	Stagnation conditions
ℓ or j	Type of chemical change
1	State of unburned gas (initial state)
2	State of unreacted gas behind a normal shock wave
3	State of gas at tail of detonation wave
∞	Free-stream conditions

IGNITION, COMBUSTION, DETONATION, AND QUENCHING OF REACTIVE MIXTURES

Three different areas of the research program have been investigated during this reporting period

1 April 1978 through 31 March 1979

I. TRANSITION FROM DEFLAGRATION TO DETONATION

A. INTRODUCTION

The distance which a deflagration wave, traversing a combustible gas mixture in a closed vessel or an unconfined cloud, must travel before a detonation wave is formed is of great practical importance. Although in some cases detonative combustion is desirable (such as in fuel-air explosions, supersonic ramjets, and high-efficiency combustion chambers), frequently it is not wanted as in accidental fires of fuel-air mixtures, and in unsteady combustion causing large pressure fluctuation (combustion instability) in the combustion chambers of rocket engines. For the design of devices which involve supersonic combustion it is extremely important to have criteria which can be used to predict the distance a deflagration wave must travel to become a detonation wave. Although numerous investigations have provided us with a fairly good picture of the mechanism of transition, there are no expressions which permit us to predict the detonation induction distance of a combustible gas mixture. The research and the experimental measurements described in the following sections of this report are carried out to provide theoretical or empirical expressions for predicting induction distances in fuel oxidizer mixtures.

B. DETONATION, INDUCTION DISTANCES OF HYDROGEN-OXYGEN-INERT GAS MIXTURES

In previous experiments[1] with M.E.R. mixtures of hydrogen and oxygen ($H_2 + \frac{1}{2} O_2$) and hydrogen + air we observed that the induction distances of these mixtures are reduced drastically when the initial temperature of the combustible gas mixture is of the order of 100 K (see Table I). Considering the fact that the normal burning speed of these mixtures decreases with decreasing temperature it is difficult to give the exact reason for this kind of a temperature effect on the induction distance. Examining the various factors which might affect the induction distance, we note that the density of the gas mixtures was inversely proportional to the temperature in these experiments since a pressure of 1 atm was maintained in all experiments. Thus the thermal energy released per unit volume of the mixture in the low-temperature mixture is greater than in the mixture at room-temperature. Furthermore the higher density of the unburned gas mixture offers a greater resistance to the expanding burned gas. Because of this resistance the combustion occurs more nearly at constant volume than at constant pressure (no resistance) and consequently a rather marked increase in pressure occurs right at the beginning of the combustion. Such large and rapid pressure rises have indeed been observed at low

Table I. Induction Distances in $H_2 + \frac{1}{2} O_2$ and $H_2 + \frac{1}{2} O_2 + 1.88 N_2$ Mixtures at 300 and 123 K

Mixture	Induction Distances	
	300 K	123 K
$H_2 + \frac{1}{2} O_2$	143 cm	15 cm
$H_2 + \frac{1}{2} O_2 + 1.88 N_2$	>600 cm	230 cm

initial temperatures. Although similar and even greater density changes can be produced by raising the initial pressure at a fixed temperature, the effect on the induction distance is not as drastic. The results of previous measurements[2] with hydrogen-oxygen-inert gas mixtures, $H_2 + \frac{1}{2} O_2 + X$, where $X = N_2$, or He, or A, are shown in Table II. The effect of pressure on the $H_2 + \frac{1}{2} O_2 + N_2$ mixture is shown in Table III. According to these measurements the induction distances decrease only moderately with increasing pressure.

From theoretical considerations it has been found that the induction distance is a function of the normal flame speed of the combustible mixture, the acceleration of the flame propagation, and the speed of sound of the unburned gas. For a given fuel-oxidizer mixture the flame front accelerates for three reasons; i.e., (1) the temperature of the unburned gas is increased, (2) the motion of the gas mixture ahead of the flame front becomes turbulent, and (3) the pressure of the unburned gas ahead of the flame is increased. Whereas the rate of flame propagation is always increased with increasing temperature and turbulence, an increase in pressure produces an increase in flame speed only in fuel-oxygen mixtures. The flame speeds of fuel-air mixtures either are practically independent of pressure or decrease slightly at higher pressures. The role of turbulence is most difficult to assess. The experiments with hydrogen-oxygen mixtures at low temperatures, at which the flame speeds are small, seem to indicate that the role of turbulence is secondary. At the short induction distances not much turbulence may have been generated.

Although flame acceleration appears to have a great effect on the transition from deflagration to detonation, a more important aspect seems to be the rate at which the pressure increases behind the flame front. For instance, hydrogen-oxygen mixtures at room temperature have rather large induction distances, whereas acetylene-oxygen mixtures whose burning velocities are practically the same have much shorter induction distances. The major difference between the two mixtures is the density. The density of an M.E.R. acetylene-oxygen mixture is 2.5 times as great as that of an

Table II. Induction Distances in $H_2 + \frac{1}{2} O_2 + nX$ Mixtures at 1 and 5 atm Initial Pressure and $T_1 = 313.15$ K (Length of Tube = 350 cm; I.D. = 5 cm)

nX	P_1 (atm)	X_{ind} (cm)
$\frac{1}{2} N_2$	1	230
	5	120
$1 N_2$	1	>350
	5	250
$\frac{1}{4}$ He	1	180
	5	70
$\frac{1}{2}$ He	1	240
	5	110
$\frac{1}{2}$ A	1	180
	5	45
1 A	1	240
	5	115
$\frac{1}{4} CO_2$	1	240
	5	115

Table III. Induction Distance as a Function of Pressure (T_1 = 300 K)

	X_{ind}		
Pressure / Mixture	0.5 atm	1 atm	2 atm
$H_2 + \frac{1}{2} O_2 + N_2$	475 cm	325 cm	270 cm

M.E.R. hydrogen-oxygen mixture. Although the combustion enthalpy of a unit volume of the acetylene-oxygen mixture is also much greater than that of the hydrogen-oxygen mixture, the difference may not be significant since both mixtures have practically the same flame temperature so that a constant volume combustion produces very nearly the same pressure ratio of ~10 when the initial gas temperature is 300 K. The formation of higher pressures during the initiation of the detonation wave results from an energy transfer because work is done by the burnt gas on the gas behind the shock wave preceding the flame. The role of density is also evident when we compare the induction distances of $H_2 + \frac{1}{2} O_2 + nA$ mixtures with those of $H_2 + \frac{1}{2} O_2 + nHe$ mixtures, as shown in Table II. The energy density in all three mixtures is the same. The burning speeds of $H_2 + \frac{1}{2} O_2 + nHe$ are much greater than those in $H_2 + \frac{1}{2} O_2 + nA$ mixtures, whereas those in the mixture containing nitrogen are slightly smaller (Fig. 1).

The induction distances with argon are much smaller than those in the mixtures with nitrogen or helium. That the induction distance in mixtures containing nitrogen is practically identical with that in the mixture with helium can be explained on the basis of the lower adiabatic combustion as well as detonation temperature of the mixture containing nitrogen. The large induction distance of $H_2 + \frac{1}{2} O_2 + CO_2$ mixtures in spite of their high density must be attributed to the interaction between CO_2, H_2, and H_2O. For the same reason the flame speed and flame temperature of this mixture are also very low. Experiments with these mixtures at low-temperature will be carried out in the near future.

C. FLAME SPEEDS OF HYDROGEN-OXYGEN-INERT GAS MIXTURES

To determine the qualitative and quantitative relationships between the flame parameters and the induction distances of various combustible gas mixtures, flame speeds are being measured for several hydrogen-oxygen-inert gas mixtures with different amounts of additive gas and over as wide a temperature range as possible (100 to 400 K provided condensation of the additive gas does not occur). A special nozzle burner with a sine curve contour is used for these measurements to obtain laminar flames with nearly straight flame cones even at Reynolds numbers up to 10,000. The measurements are extremely reproducible. Results obtained so far are shown in Fig. 1. It is interesting to note that $H_2 + \frac{1}{2} O_2 +$ argon mixtures have practically the same flame speeds as $H_2 + \frac{1}{2} O_2 +$ nitrogen mixtures in spite of the large physical and chemical differences between these two additives.

D. EFFECT OF INITIAL TEMPERATURE ON WAVE SPEED OF, AND FINAL PROPERTIES BEHIND C.J. DETONATION WAVES IN THE M.E.R. MIXTURE OF HYDROGEN WITH AIR

The wave speed, gas speed, pressure, temperature, and density were calculated for the M.E.R. (maximum energy release; molar ratio of hydrogen to oxygen = 2:1) mixture of hydrogen and air at various initial

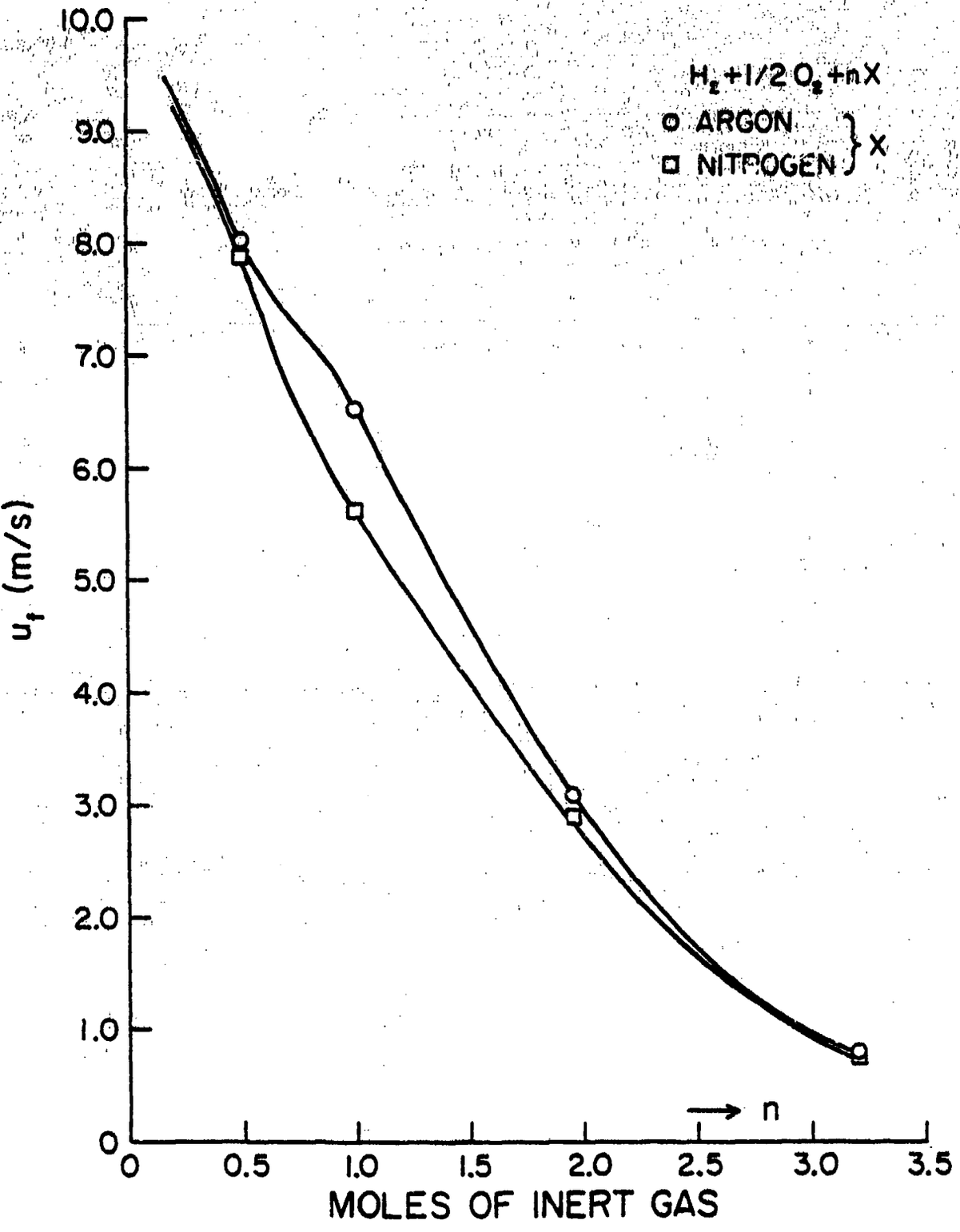

Fig. 1 - Flame Speed (u_f) vs Moles of Inert Gas Added to $H_2 + \frac{1}{2}\,O_2$

temperatures (T_1 = 100 to 473 K) and initial pressures (p_1 = 1 to 100 atm). The results are shown in Figs. 2, 3, 4, 5, and 6. According to these calculations the wave speed is inversely proportional to the temperature of the unburned gas but proportional to its pressure (Fig. 2), whereas the gas speed increases very slightly with increasing initial temperature and pressure (Fig. 3). Although the final temperature increases with increasing initial temperature, the increase is much less than that of the initial gas temperature. This behavior is probably due to the less efficient energy transfer from burned gas to the gas behind the wave which will be discussed in the next section. The increase in T_3 caused by an increase in p_1 is due to a reduction in dissociation of the combustion gas molecules (Fig. 4). Because of the importance of turbulence on the rate of flame propagation the effect of pressure on the speed of the detonated gas is shown in Fig. 5, which clearly reveals that u_3 increases only very slightly with pressure although the induction distances of almost all combustible mixtures decrease rather markedly with a rise in pressure of the initial gas. The most significant observation is the large increase of the pressure of the detonated gas as the temperature is lowered (Fig. 6). On the other hand, a change of the initial pressure hardly affects the pressure ratio. As shown in the next section the relative amount of energy transferred from the downstream burned gas to the gas behind the normal shock wave preceding the combustion zone is directly proportional to the pressure ratio; e.g.,

$$\frac{\Delta h^\circ}{R_1 T_1} = \left(\frac{p_3}{p_1} - 1\right) ,$$

where $R_1 = \frac{\mathcal{R}}{m_1}$.

Although it is tempting to relate the drastic reductions of the induction distances at very low initial temperature of the unburned gas to the energy transfer, no definite statement can be made at this time because the observed pressures of the detonated gas mixture at low initial temperatures were found to be much lower than the calculated values. Therefore, more experiments with different combustible gas mixtures at low initial temperatures are necessary to establish a quantitative relationship between mixture properties and detonation induction distance.

II. INVESTIGATION OF THE MECHANISM OF FLAME QUENCHING

The following topics were investigated:

(1) The effect of salt coatings--thick coatings of salt were obtained by painting solutions of potassium chloride, sodium bicarbonate, and tribase potassium phosphate on both surfaces of the quenching plates. Thick layers (about 0.16 cm) of the salts were used so that the flame could react chemically with the salt during the prolonged contact of the flame with the quenching plate surfaces. It was observed

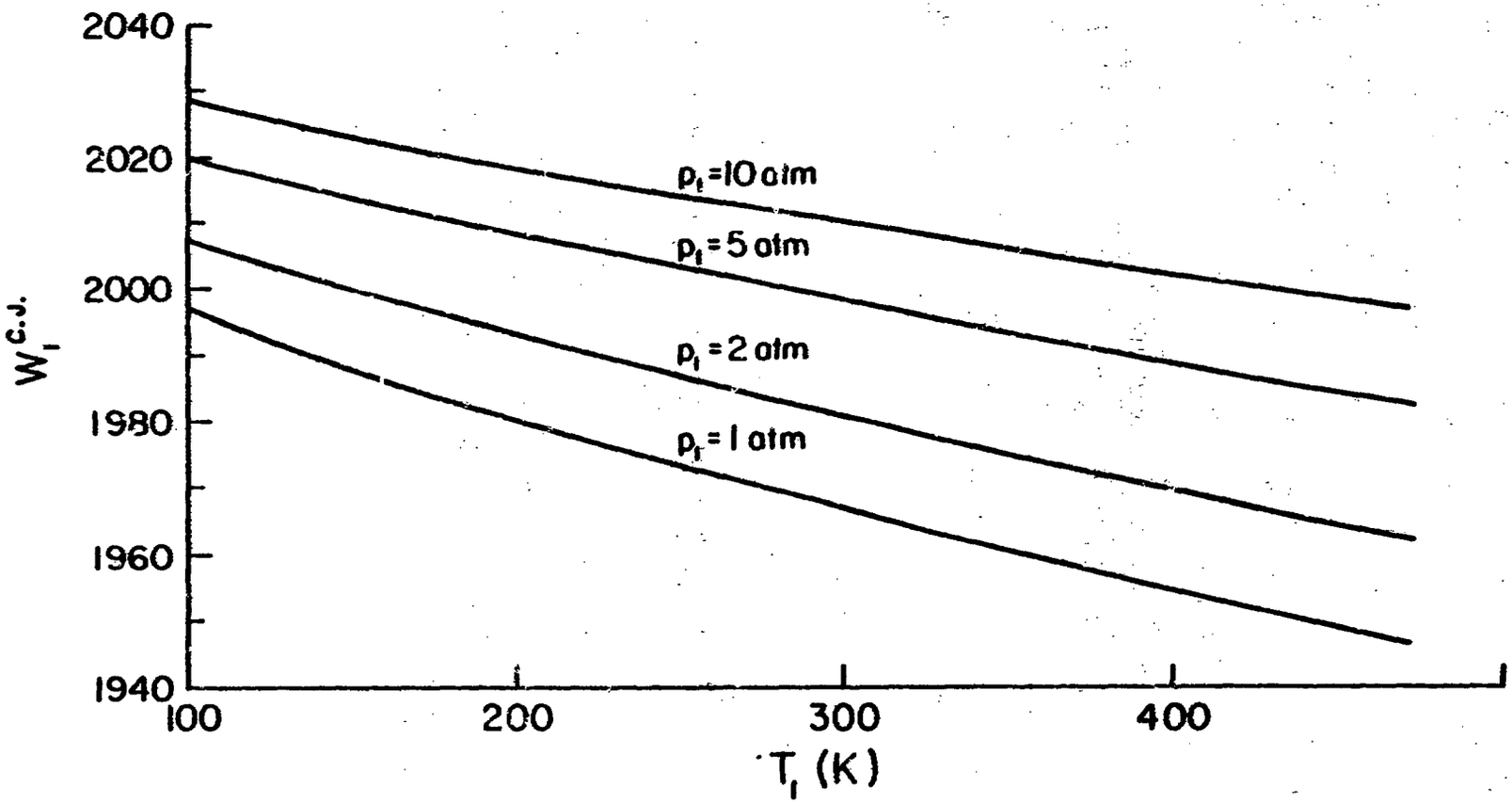

Fig. 2 - Calculated Wave Speed, $w_1^{C.J.}$, of Detonating H_2 - air (M.E.R.) Mixture at Various Values of T_1 and p_1

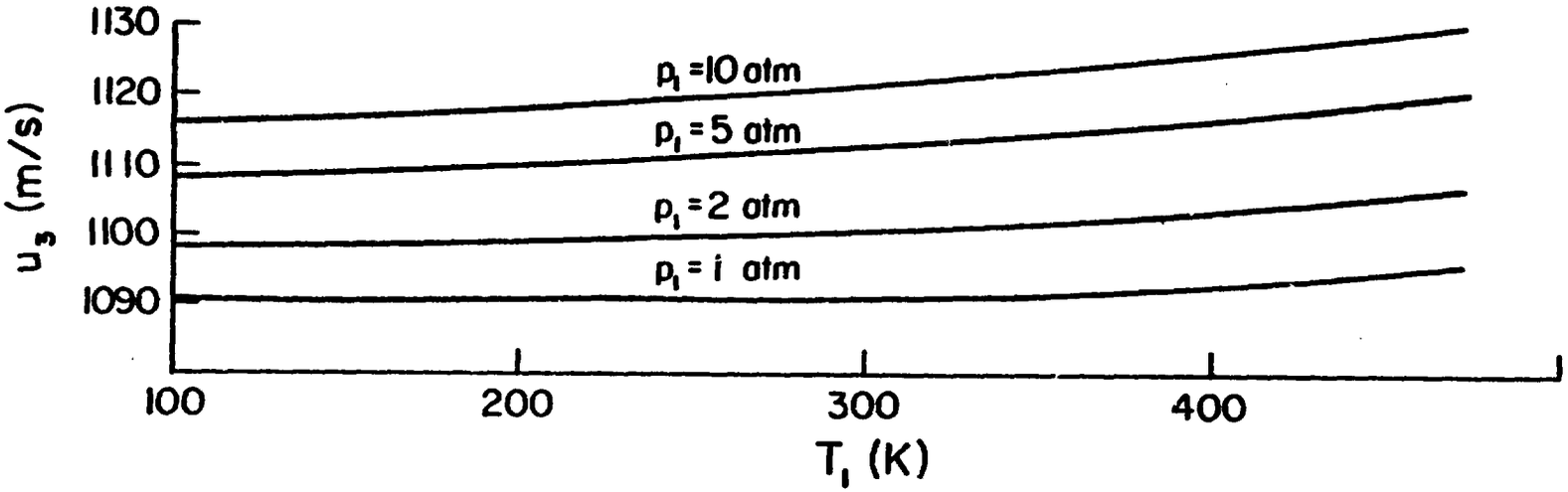

Fig. 3 - Calculated Gas Speed, u_3, of Detonated H_2 - air (M.E.R.) Mixture at Various Values of T_1 and p_1

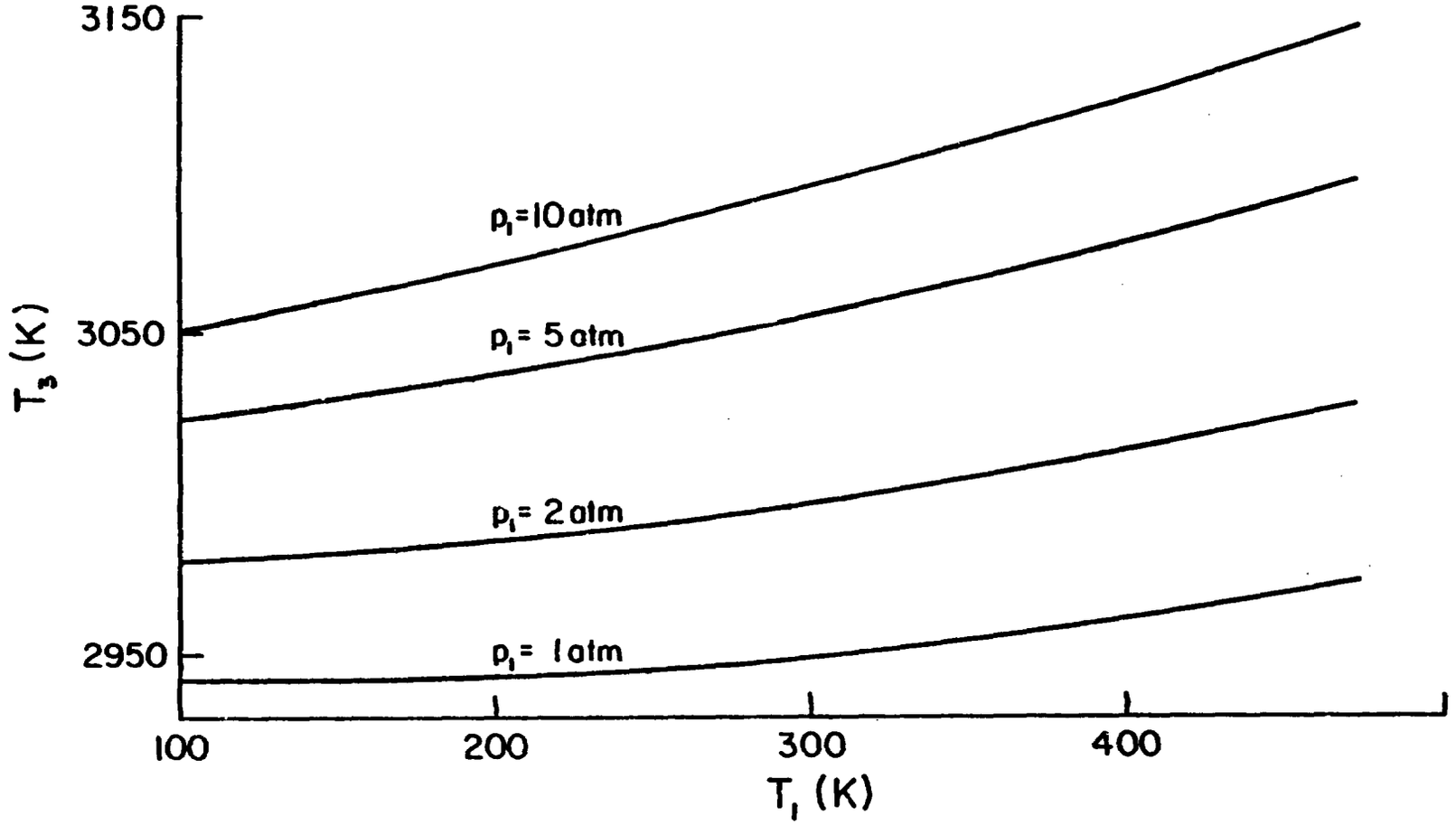

Fig. 4 - Calculated Temperature of Detonated H_2 - air (M.E.R.) Mixture at Various Values of T_1 and p_1

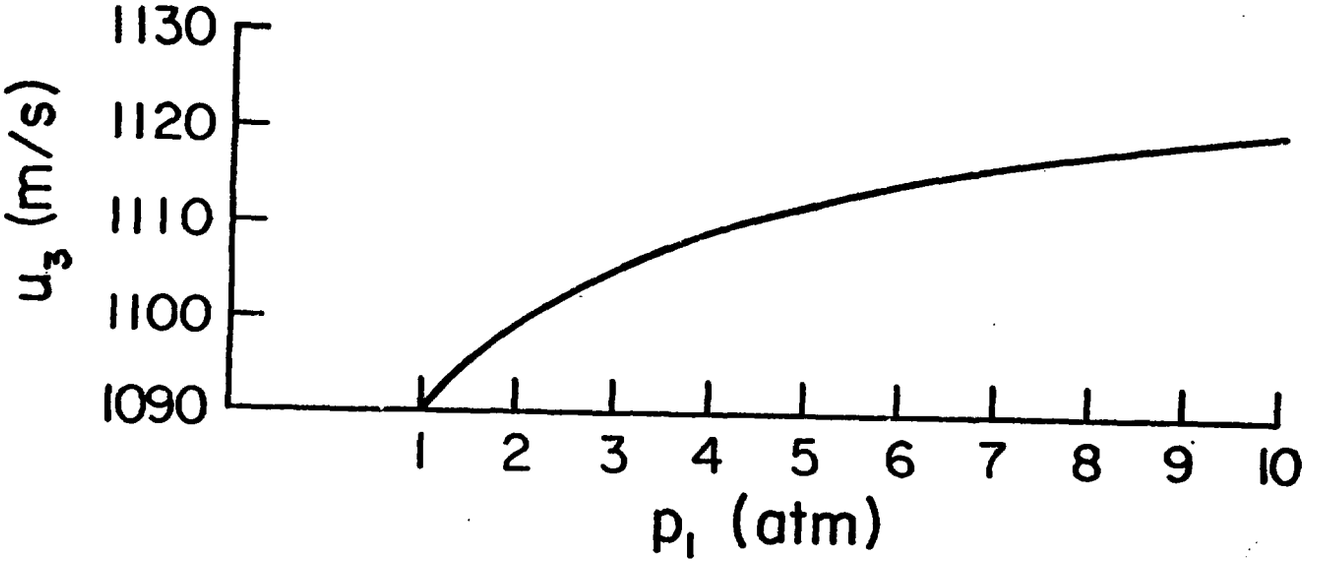

Fig. 5 - Calculated Gas Speed, u_3, of Detonated H_2 - air (M.E.R.) Mixture as a Function of the Initial Pressure, p_1 (T_1 = 273.15 K)

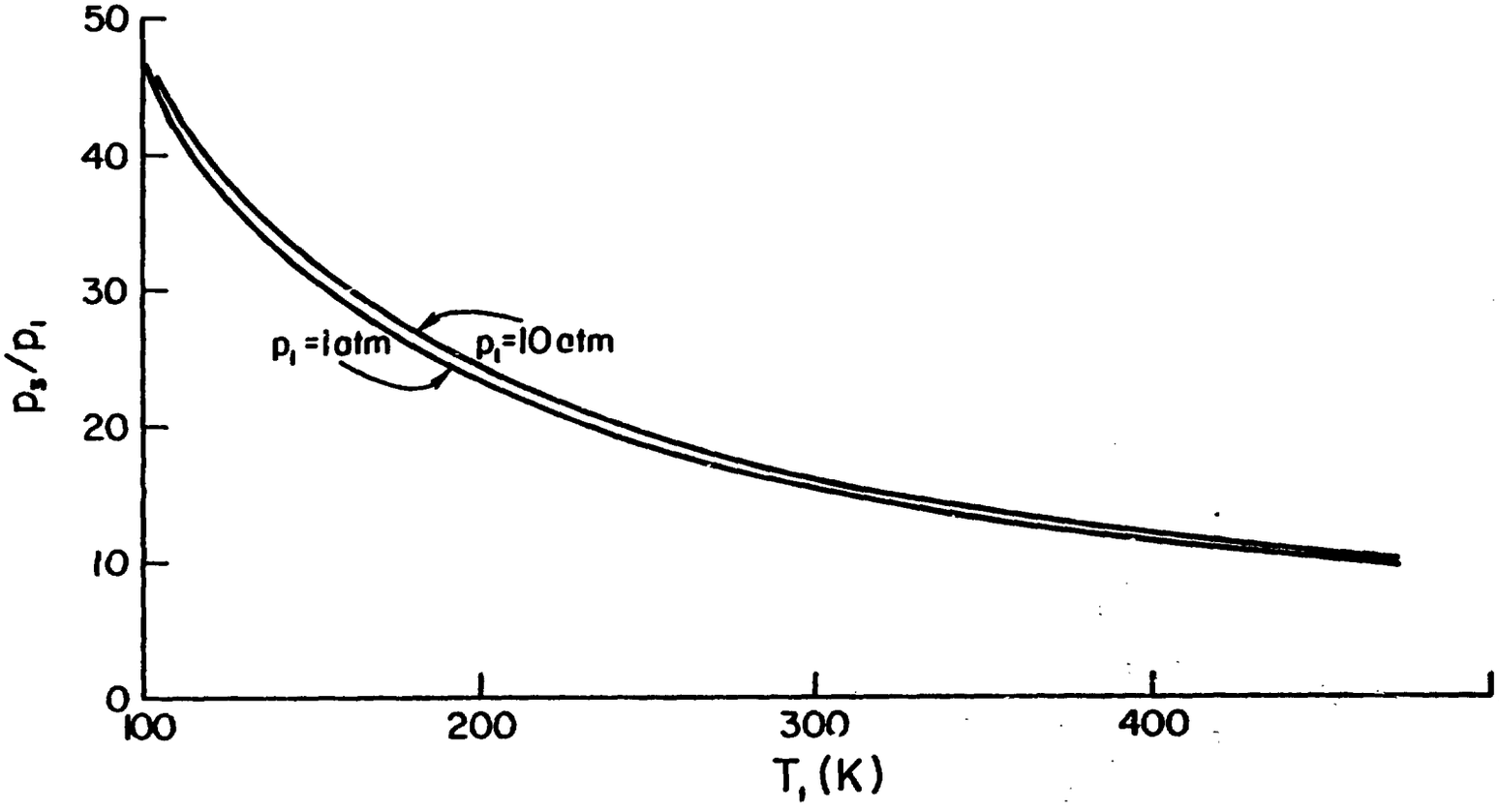

Fig. 6 - Calculated Pressure of Detonated H_2 - air (M.E.R.) Mixture at Various Values of T_1 and p_1

that salt coatings of potassium chloride and sodium bicarbonate vanish rather rapidly when exposed to the flame, whereas the coating of tribase potassium phosphate remains on the plate surface much longer. It was found that the appearance of the flames of methane-air, methane-oxygen, acetylene-air, and hydrogen-air mixtures was affected by the three salts although the quenching distances were hardly changed. Therefore, it can be concluded that these salt coatings do not promote the flame quenching process.

(2) The effect of gas speed on quenching distance--further experiments were performed by increasing the volume flow rate of the unburned gas to 200 cc/s (twice the volume flow rate used in previous experiments). For the gas mixtures considered (i.e., methane-air, methane-oxygen, acetylene-air, and hydrogen-air), the quenching distances remain unchanged. Consequently, it can be concluded that for laminar flames the measured quenching distances are independent of the initial gas speed.

(3) The mathematical expression developed for the flame quenching distance, d_Q; i.e.,

$$d_Q = \frac{4\lambda h + 2D_{mix} c_p b}{c_p b u_F \alpha},$$

where

λ = thermal conductivity of the gas mixture at average flame temperature,

h = height of the quenching plate,

D_{mix} = diffusion coefficient of the gas mixture at average flame temperature,

c_p = specific heat at constant pressure at an average flame temperature,

b = short side of the burner port,

u_F = flame speed, and

α = geometrical factor of the order of unity,

suggests that the quenching distance should be affected by

(a) the width b, of the burner port and

(b) the height of the quenching plate, h.

In order to study the effect of the width of the burner opening, experiments were performed with methane-air flames by using a new burner whose width was two times that of the original burner; i.e., 0.34 cm. The measurements reveal that the quenching distance is slightly reduced (of the order of 10 percent) when b is increased.

Then experiments were performed with the original burners after the height of the quenching plates, h, was increased two times the original height (from 2.5 to 5 cm). These results showed that for the gas mixtures examined, the quenching distances are independent of the quenching plate height, h.

(4) In order to determine the relationship between the quenching distance measured in our laboratory and those established by an entirely different technique by previous investigators, experiments were performed to measure that distance between the quenching plates (once the quenching is established) where the flame burning on the top of these plates just settles down suddenly; i.e., flashes back. To determine this point the quenching plates (made of copper) were moved apart very slowly. Sudden flash-back, however, did not occur; the flames entered gradually and slowly descended between the two plates. Further studies are necessary, probably with temperature-controlled plates, to explain this unexpected behavior.

(5) Further experiments were performed by closing the side openings of the copper plates. In this way a rectangular enclosure of the quenching zone was formed. It was found that at a certain distance between the plates the flames burning at the top of these plates suddenly jumped down to the burner tip when the plates were moved apart slowly. When copper plates were used all around, it was not possible to see where the flame was quenched and furthermore it was not possible to see whether the quenching process was sudden. In order to observe the flash-back point, glass plates were employed to form the enclosure. It was found that the flame entered the burner suddenly and when the plates were moved together, at a certain distance the flame jumped to the top of the plates. The distance between the plates at which the flame suddenly leaves the burner and jumps to the top of the plates was measured for methane-air flames. The results are compared below.

% Methane	Quenching Distance without Glass Plates (mm)	Quenching Distance with Glass Plate Enclosure (mm)
7.0	2.43	3.68
8.0	2.22	3.28
9.5	2.10	3.16
11.0	2.25	3.72
12.0	2.41	5.30

It must be concluded that the true quenching distance is given by the values obtained with the enclosure of the narrow side of the quenching space.

III. NEW CALCULATION TECHNIQUES

A. CALCULATION OF DETONATION PARAMETERS AND ENERGY TRANSFER

For the present calculations we consider the mixtures

$$H_2 + \tfrac{1}{2} O_2 + \nu_y Y$$

where Y = argon, helium, nitrogen, or carbon-dioxide. For estimated values of T_3 and p_3 and specified values of T_1, p_1, ν_y, and Y the $\eta_{i,3}$ (η_{H_2O}, η_{O_2}, η_{OH}, η_{H_2}, η_O, η_H, η_{He}, η_A, η_{N_2}, η_{NO}, η_{CO_2}, and η_{CO}) are calculated according to the technique explained in Section III-B.

Since the adiabatic flame temperature at constant volume $\left(T_3^{dv=0}\right)$ is the lowest temperature a supersonic combustion wave can attain, it is advisable to calculate this temperature first. In this case we have $w_1 = w_3 = \infty$ and $u_3 = 0$. To find the pressure, p_3, which is compatible with the assumed temperature, T_3^{est}, we use the condition that

$$p_3^{calc} = p_1 \cdot \frac{T_3}{T_1} \cdot \frac{m_1}{m_3} \quad , \quad \text{when } \frac{v_3}{v_1} = 1 \ ,$$

where $m_3 = \sum_i \eta_{i,3} m_i$.

Since for a given T_3 the molecular mass m_3 increases as p_3 is increased (less dissociation) and vice versa, p_3^{calc} will be smaller than the correct

value when p_3^{est} is larger than the correct value and vice versa. Hence a subsequent estimate of p_3 is obtained from the interpolation formula

$$p_3^{est(n)} = (1 - \xi)\, p_3^{est} + \xi p_3^{calc} ,$$

where $0 < \xi < 1$, usually 0.5.

The iterations are repeated until

$$100 \cdot \left| \frac{p_3^{calc(n)} - p_3^{est(n)}}{p_3^{calc(n)}} \right| < \Delta p_3 = 0.001\% .$$

After the correct value of p_3 has been calculated, the energy equation is used to calculate the correct temperature T_3. For combustion at constant volume we have

$$e_f^{T_3} = e_f^{T_1}$$

which can be written in terms of the reduced formation enthalpies as follows: first we write

$$\frac{\mathcal{R}T_3}{m_3} \left(\frac{e_f}{RT}\right)^{T_3} = \frac{\mathcal{R}T_1}{m_1} \left(\frac{e_f}{RT}\right)^{T_1} ;$$

'solving' for T_3 we obtain

$$T_3^{calc} = T_1 \cdot \frac{m_3}{m_1} \cdot \frac{\left(\frac{e_f}{RT}\right)^{T_1}}{\left(\frac{e_f}{RT}\right)^{T_3}} .$$

Since usually only formation enthalpies are tabulated we use the relationships $e = h - pv$ and $E = H - \mathcal{R}T$ (thermally perfect gas) and obtain

$$T_3^{calc} = T_1 \cdot \frac{m_3}{m_1} \frac{\left(\frac{h_f}{RT}\right)^{T_1} - 1}{\left(\frac{h_f}{RT}\right)^{T_3} - 1} ,$$

where $\left(\frac{h_f}{RT}\right)^{T} = \sum \eta_i \left(\frac{H_f}{\mathcal{R}T}\right)_i^{T}$

and

$$\left(\frac{H_f}{\Re T}\right)_i^T = \left(\frac{H-E_o}{\Re T}\right)_i + \frac{\Delta E_{o,i}}{\Re T} .$$

The $\Delta E_{o,i} \equiv E_{o,i} - \sum_{el} \nu_{el}^{(i)} E_{o,el}$ may be considered as the formation energies (or enthalpies) of the species i at T = OK. When $T_3^{calc} \neq T_3^{est}$ the calculations are repeated with improved estimates according to the equation

$$T_3^{est(n)} = T_3^{est(n-1)} - \Delta$$

where

$$\Delta = \frac{T_3^{est(n-1)}}{m_3}\left[\left(\frac{h_f}{RT}\right)^{T_3^{est(n-1)}} - 1\right] - \frac{T_1}{m_1}\left[\left(\frac{h_f}{RT}\right)^{T_1} - 1\right]$$

until $$100 \cdot \left|\frac{T_3^{est(n)} - T_3^{calc(n)}}{T_3^{est(n)}}\right| < 0.001\% .$$

Now we can proceed to calculate detonative combustion parameters. For assumed values of $T_3 (T_3 > T_3^{d\nu=0})$ and $p_3 (p_3 > p_3^{d\nu=0})$ first we must calculate again the $\eta_{i,3}$. To find the correct pressure for the assumed temperature we 'solve' for p_3 from the energy equation which yields

$$p_3^{calc} = p_1 \left[2 \cdot \frac{\frac{T_3}{T_1} \cdot \frac{m_1}{m_3}\left(\frac{h_f}{RT}\right)^{T_3} - \left(\frac{h_f}{RT}\right)^{T_1}}{1 + \frac{T_3}{T_1} \cdot \frac{p_1}{p_3} \cdot \frac{m_1}{m_3}} + 1\right] .$$

If $p_3^{calc} \neq p_3^{est}$, the calculations are repeated with improved estimates,

$$p_3^{est(n)} = (1 - \xi)\, p_3^{est(n-1)} + \xi p_3^{calc(n-1)} ,$$

until $$100 \cdot \left|\frac{p_3^{est(n)} - p_3^{calc(n)}}{p_3^{calc(n)}}\right| < \Delta p_3 = 0.0001\% .$$

Any compatible pair of T_3 and p_3 values represents a solution of the Hugoniot equation and thus a supersonic combustion wave. We have a weak

detonation when the selected temperature, T_3, is greater than $T_3^{dv=0}$ but smaller or just equal to $T_3^{C.J.}$, the temperature of the so-called Chapman-Jougnet detonation wave which is characterized by the condition $w_3 = w_{a,3}$. Weak detonation waves involve no shock transitions. When $T_3 > T_3^{C.J.}$, we have a strong detonation wave in which a subsonic combustion wave occurs behind a normal shock wave which traverses the unburned gas mixture at the speed w. For strong detonation waves we have $w_3 < w_{a,3}$.

To calculate the wave speed and the conditions behind the wave of a Chapman-Jougnet detonation, which is the one which occurs as a traveling wave, we make use of the condition that at the tail of the wave the wave speed, w_3, is equal to the speed of sound in this gas, $w_{a,3}$. This condition can be used to develop the following equation for a calculated value of T_3:

$$T_3^{calc} = T_1 \cdot \frac{\frac{m_3}{m_1}\left(\frac{h_f}{RT}\right)^{T_1}}{\left(\frac{h_f}{RT}\right)^{T_3^{est}} - \frac{1}{2}\gamma_{eff}^{T_3^{est}}\left[\left(\frac{v_1}{v_3}\right)^2 - 1\right]}, \qquad (1)$$

where

$$\gamma_{eff}^{T_3} = \frac{\sum_i \eta_{i,3}\left(\frac{C_p}{\mathcal{R}}\right)_i^{T_3} + \left|\frac{\Delta H^{(\ell)}}{\mathcal{R}T}\right|\left[a_{\ell,j}\right]^{-1}\left\{\frac{\Delta H^{(j)}}{\mathcal{R}T}\right\}}{\sum_i \eta_{i,3}\left(\frac{C_p}{\mathcal{R}}\right)_i^{T_3} - 1 + \left|\frac{\Delta H^{(\ell)}}{\mathcal{R}T} - \Delta\nu^{(\ell)}\right|\left[b_{\ell,j}\right]^{-1}\left\{\frac{\Delta H^{(j)}}{\mathcal{R}T} - \Delta\nu^{(j)}\right\}} \cdot$$

$$\frac{1 + \left|\frac{\Delta H^{(\ell)}}{\mathcal{R}T} - \Delta\nu^{(\ell)}\right| \cdot \left[b_{\ell,j}\right]^{-1} \cdot \left\{\Delta\nu^{(j)}\right\}}{1 + \left|\frac{\Delta H^{(\ell)}}{\mathcal{R}T}\right| \cdot \left[a_{\ell,j}\right]^{-1} \cdot \left\{\Delta\nu^{(j)}\right\}},$$

and where

$$\frac{\Delta H^{(\ell)}}{\mathcal{R}T} = \sum_i \nu_i^{(\ell)}\left(\frac{H_f}{\mathcal{R}T}\right),$$

$$\Delta\nu^{(\ell)} = \sum_i \nu_i^{(\ell)} \qquad \Delta\nu^{(j)} = \sum_i \nu_i^{(j)},$$

$$b_{\ell,j} = \sum_i \frac{\nu_i^{(\ell)} \cdot \nu_i^{(j)}}{\eta_{i,3}}, \text{ and}$$

$$a_{\ell,j} = b_{\ell,j} - \Delta\nu^{(\ell)} \cdot \Delta\nu^{(j)} .$$

These parameters must be calculated for the estimated temperature, T_3^{est}. When $T_3^{calc} \neq T_3^{est}$ the calculations are repeated with an improved estimate which is obtained from the following expression:

$$T_3^{est(n)} = T_3^{est(n-1)} - \Delta$$

where

$$\Delta = \frac{T_3^{est(n-1)}}{m_3} \cdot \left(\frac{h_f}{RT}\right)^{T_3^{est(n-1)}} - \frac{T_1}{m_1} \cdot \left(\frac{h_f}{RT}\right)^{T_1} .$$

The iterations are continued until

$$100 \cdot \left| \frac{T_3^{est(n)} - T_3^{calc(n)}}{T_3^{est(n)}} \right| < 0.001\% .$$

After the correct temperature has been determined the speed of the detonation wave is calculated by means of the following equation:

$$w_1^{C.J.} = \left[\frac{RT_1}{m_1} \cdot \frac{\frac{p_3}{p_1} - 1}{1 - \frac{T_3}{T_1} \cdot \frac{p_1}{p_3} \cdot \frac{m_1}{m_3}} \right]^{1/2} .$$

Although these calculations produce data which describe only the steady-state motion of the wave and, therefore, cannot be used directly to calculate the induction distance, it appears that the pressure ratio, $\frac{p_3}{p_1}$, and the energy transfer from the burned gas to the gas behind the wave may be related to the magnitude of the induction distance as determined in these calculations. The amount of energy transfer can be calculated as follows: The stagnation enthalpy of the unburned gas relative to a laboratory-fixed coordinate system is h^{T_1} and that of the gas at the tail of the wave is $h^{T_3} + \frac{u_3^2}{2}$. Hence the amount of energy transferred is

$$\Delta h^{\circ} = h^{T_3} + \frac{u_3^2}{2} - h^{T_1} = h_f^{T_3} + \frac{(w_1 - w_3)^2}{2} - h_f^{T_1} .$$

Relative to the wave we have

$$h_f^{T_3} + \frac{w_3^2}{2} = h_f^{T_1} + \frac{w_1^2}{2}$$

and thus

$$h_f^{T_3} - h_f^{T_1} = \frac{w_1^2 - w_3^2}{2} .$$

Substitution leads to

$$\Delta h^o = \frac{w_1^2 - w_3^2}{2} + \frac{w_1^2 + w_3^2}{2} - w_1 w_3 = w_1^2 - w_1 w_3$$

or

$$\Delta h^o = w_1^2 \left(1 - \frac{w_3}{w_1}\right) = \frac{\Re T_1}{\mathfrak{M}_1} \frac{\frac{p_3}{p_1} - 1}{1 - \frac{v_3}{v_1}} \left(1 - \frac{v_3}{v_1}\right) ,$$

so that

$$\frac{\Delta h^o}{\left(\frac{\Re T_1}{\mathfrak{M}_1}\right)} = \frac{p_3}{p_1} - 1 .$$

This expression shows that the relative energy transfer, $\frac{\Delta h^o}{\left(\frac{\Re T_1}{\mathfrak{M}_1}\right)}$, is proportional to the pressure ratio, $\frac{p_3}{p_1}$. The relationship between these parameters and the induction distance will be examined in future experiments.

B. CALCULATION OF PERFORMANCE OF SUPERSONIC RAMJET ENGINE

The analysis includes the following processes and engine parameters:

1. Diffusion from the Free-Stream Air Speed, u_∞, to a Specified Value, u_{DE}, at the Diffuser Exit or the Combustion Chamber Inlet $\left(u_{c,1} = u_{DE}\right)$.

   a. The diffuser is assumed to be isentropic.

      1. The decelerated airflow is subsonic

      2. The decelerated airflow is supersonic

   b. A normal shock wave is formed at the inlet of the diffuser and subsonic diffusion to u_{DE} follows.

   c. The deceleration of the incoming airflow occurs first via an oblique shock wave on a wedge, then via a normal shock wave which is followed by a subsonic diffusion to u_{DE}.

2. Fuel is Added to the Air Stream Tangentially and Burned in a Constant Area Duct $A_c = A_{DE} + A_{FUEL}$.

   a. The airflow entering the combustion chamber is subsonic.

   b. The airflow entering the combustion chamber is supersonic.

      (1) Combustion occurs without any shock waves (stationary weak detonation wave)

      (2) Combustion is preceded by a normal shock wave (stationary strong detonation wave)

3. Expansion Through Exhaust Nozzle

   a. The expansion is isentropic: convergent-divergent nozzle with $p_e = p_a (M_e > 1)$.

   b. The nozzle consists of a convergent section only $(M_e = 1)$ $p_e > p_a$. Flow-through nozzle is assumed to be isentropic but expansion from p_e to p_a outside the nozzle is accompanied by a rather large increase in entropy.

4. Calculation of Important Cross-Sectional Areas; Only Relative Values, Referenced to the Inlet Area A_i, Will be Given.

   a. A_{Dt} = throat area of diffuser for the case of isentropic diffusion to a subsonic speed u_{DE}.

   b. A_{DE} = area of diffuser exit.

   c. $A_c = A_{DE} + A_{FUEL}$ = area of combustion chamber.

   d. A_{Nt} = throat area of exhaust nozzle.

   e. A_{NE} = area of exit of convergent-divergent exhaust nozzle.

SPECIFICATIONS

FREE STREAM CONDITIONS = CONDITIONS OF AMBIENT AIR:

$\underline{\underline{T_\infty}}$, $\underline{\underline{p_\infty}}$, $\underline{\underline{u_\infty}}$ (or M_∞)

'AIR' = $1O_2 + 3.76\ N_2$

$$m_{air} = 28.85297479 \text{ kg/kmol}$$

FUEL: $CH_{2 \cdot \nu_{H_2}}$ $\underline{\underline{\nu_{H_2}}}$ = (to be specified

$$m_{FUEL} = (12.01 + \nu_{H_2} \cdot 2.016) \text{ kg/kmol} \equiv m_{CH_{2 \cdot \nu_{H_2}}}$$

FUEL-AIR MIXTURE: $CH_{2\nu_{H_2}} + \nu_{O_2}(O_2 + 3.76\ N_2)$

MIXTURE RATIO: $f = \dot{m}_{FUEL} / \dot{m}_{air} = m_{CH_{2\nu_{H_2}}} / 4.76\ \nu_{O_2} \cdot m_{air}$

$\underline{\underline{\nu_{O_2}}}$ = to be specified

All underlined properties and A_i (or $\dot{m}_{air}$) must be specified.

Furthermore, the thermodynamic properties of the fuel, the air and all combustion products must be available.

T_L = integer hundred nearest T but $T_L < T$.

$m_\infty = (T_L - T_\infty)/100$

$c^T_{s,i}$ = Entropy Coefficient of Species i at Temperature T.

For air at T_∞ we have

$$c^{T_\infty}_{s,air} = \frac{1}{4.76} \cdot \left\{ \left[\frac{\left(\frac{S^{p=1}}{\mathcal{R}} \right)}{\ln T} \right]_{O_2}^{T_L} \cdot (1 - m_\infty) + \left[\frac{\left(\frac{S^{p=1}}{\mathcal{R}} \right)}{\ln T} \right]_{O_2}^{T_L+100} \cdot m_\infty + 3.76 \cdot \left(\left[\frac{\left(\frac{S^{p=1}}{\mathcal{R}} \right)}{\ln T} \right]_{N_2}^{T_L} \cdot (1 - m_\infty) + \left[\frac{\left(\frac{S^{p=1}}{\mathcal{R}} \right)}{\ln T} \right]_{N_2}^{T_L+100} \cdot m_\infty \right) \right\}$$

FORMATION ENTHALPY:

$$\left(\frac{h_f}{RT}\right)_{air}^{T_\infty} = \frac{1}{4.76} \cdot \left\{ \left(\frac{H-E_o}{\mathcal{R}T}\right)_{O_2}^{T_L} \cdot (1 - m_\infty) + \left(\frac{H-E_o}{\mathcal{R}T}\right)_{O_2}^{T_L+100} \cdot m_\infty + \right.$$

$$\left. 3.76 \cdot \left(\left(\frac{H-E_o}{\mathcal{R}T}\right)_{N_2}^{T_L} \cdot (1 - m_\infty) + \left(\frac{H-E_o}{\mathcal{R}T}\right)_{N_2}^{T_L+100} \cdot m_\infty \right) \right\} .$$

$$\sum \eta_{i,\infty} \ln \eta_{i,\infty} = \frac{1}{4.76} \left\{ \ln \frac{1}{4.76} + 3.76 \ln \frac{3.76}{4.76} \right\} = \underline{-0.5140679876}$$

1.a. Isentropic Diffusion to $u_{DE}(M_{DE} < 1)$.

From the energy equation we have

$$T_{DE}^{calc} = T_\infty \cdot \frac{m_{DE}}{m_{air}} \frac{\left(\frac{h_f}{RT}\right)_{air}^{T_\infty} + \frac{1}{2} \frac{u_\infty^2 - u_{DE}^2}{R_{air} T_\infty}}{\left(\frac{h_f}{RT}\right)_{DE}^{T_{DE}^{est}, p_{DE}^{est}}} , \qquad (2)$$

where

$$\left(\frac{h_f}{RT}\right)_{DE}^{T_{DE}^{est}, p_{DE}^{est}} \equiv \sum_i \eta_{i,DE} \left(\frac{H_f}{\mathcal{R}T}\right)_i^{T_{DE}^{est}} .$$

From the entropy equation we have

$$p_{DE}^{calc} = p_\infty^{\left(\frac{m_{DE}}{m_{air}}\right)} \cdot \frac{T_{DE}^{c_s^{T_{DE}}}}{T_\infty^{\left(\frac{m_{DE}}{m_{air}}\right) \cdot c_{s,air}^{T_\infty}}} \cdot$$

$$\cdot e^{\left(\frac{m_{DE}}{m_{air}}\right) \sum_i \eta_{i,\infty} \ln \eta_{i,\infty} - \sum \eta_{i,DE} \ln \eta_{i,DE}} , \qquad (3)$$

where

$$c_s^{T_{DE}} = \sum_i \eta_{i,DE} \left[\frac{\left(\frac{S^{p=1}}{\mathcal{R}} \right)}{\ell n\, T} \right]_i^{T_{DE}} .$$

The $\eta_{i_{DE}}$ depend on T_{DE} and p_{DE}. They must be calculated by an iterative procedure. For estimated values of T_{DE} and p_{DE} (obtained from Eq. (2) and Eq. (3) with estimates of $(h_f/RT)_{DE}^{T_{DE},p_{DE}}$ and $c_s^{T_{DE}}$; approximately $hf/RT \sim \gamma/\gamma - 1$ and $c_s \sim \gamma/\gamma - 1$) the $\eta_{i,DE}$ are calculated as follows:

STEP: (1) $$\frac{T_{DE}^{est} - T_L}{100} = \underline{\underline{m_{DE}}} ,$$

(2) $$\left[a^{(O)}(T_L) \right]^{(1-m_{DE})} \cdot \left[a^{(O)}(T_L + 100) \right]^{m_{DE}} \cdot \sqrt{T_{DE}^{est}} \cdot e^{-\frac{29685}{T_{DE}^{est}}} \cdot \left(p_{DE}^{est} \right)^{-\frac{1}{2}} = K^{(O)} ,$$

(3) $$\left[a^{(NO)}(T_L) \right]^{(1-m_{DE})} \cdot \left[a^{(NO)}(T_L + 100) \right]^{m_{DE}} \cdot e^{-\frac{10799}{T_{DE}^{est}}} = K^{(NO)} , \text{ and}$$

(4) $$\sqrt{\eta_{O_2}^{est(O)}} \approx \left[\sqrt{1 + \left(\frac{1}{2} K^{(O)} \right)^2} - \frac{1}{2} K^{(O)} \right] \cdot 0.458 ,$$

(5) $$\eta_O = K^{(O)} \cdot \sqrt{\eta_{O_2}^{est}} ,$$

(6) $$\eta_{N_2} = \left(\left(\left(K^{(NO)} \right)^2 \cdot \eta_{O_2}^{est} \cdot \frac{1}{4} + 1 - \eta_O - \eta_{O_2}^{est} \right)^{\frac{1}{2}} - K^{(NO)} \cdot \sqrt{\eta_{O_2}^{est}} \cdot \frac{1}{2} \right)^2 ,$$

(7) $\eta_{NO} = K^{(NO)} \cdot \sqrt{\eta_{N_2}} \cdot \sqrt{\eta_{O_2}^{est}}$,

(8) $\eta_{O_2}^{calc} = \left(\eta_{N_2} + \frac{1}{2}\,\eta_{NO}\right) + 3.76 - \left(\eta_O + \eta_{NO}\right) + 2$.

When $\eta_{O_2}^{calc} \neq \eta_{O_2}^{est}$ repeat Steps (5) through (8) with

(9) $\eta_{O_2}^{est(n)} = \xi \cdot \eta_{O_2}^{calc(n-1)} + (1 - \xi) \cdot \eta_{O_2}^{est(n-1)}$,

where $0 < \xi < 1$ (usually $\xi = 0.5$ but in some cases $\xi < 0.1$ to obtain convergence). Repeat iteration until

(10) $100 \cdot \left| \dfrac{\eta_{O_2}^{calc(n)} - \eta_{O_2}^{est(n)}}{\eta_{O_2}^{calc(n)}} \right| < \Delta\eta_{O_2} = 0.00001\%$.

Then calculate

(11) $\mathcal{M}_{DE} = \mathcal{M}_O \cdot \left(2\eta_{O_2} + \eta_O + \eta_{NO}\right) + \mathcal{M}_N \cdot \left(2\eta_{N_2} + \eta_{NO}\right)$

(12) $c_s^{T_{DE}} = \eta_{O_2} \cdot \left\{ \left[\dfrac{\left(\frac{S^{p=1}}{\mathcal{R}}\right)}{\ell n\, T} \right]_{O_2}^{T_L} \cdot \left(1 - m_{DE}\right) + \left[\dfrac{\left(\frac{S^{p=1}}{\mathcal{R}}\right)}{\ell n\, T} \right]_{O_2}^{T_L+100} \cdot m_{DE} \right\} +$

$+ \eta_O \cdot \left\{ \left[\dfrac{\left(\frac{S^{p=1}}{\mathcal{R}}\right)}{\ell n\, T} \right]_{O}^{T_L} \cdot \left(1 - m_{DE}\right) + \left[\dfrac{\left(\frac{S^{p=1}}{\mathcal{R}}\right)}{\ell n\, T} \right]_{O}^{T_L+100} \cdot m_{DE} \right\} +$

$+ \eta_{N_2} \cdot \left\{ \left[\dfrac{\left(\frac{S^{p=1}}{\mathcal{R}}\right)}{\ell n\, T} \right]_{N_2}^{T_L} \cdot \left(1 - m_{DE}\right) + \left[\dfrac{\left(\frac{S^{p=1}}{\mathcal{R}}\right)}{\ell n\, T} \right]_{N_2}^{T_L+100} \cdot m_{DE} \right\} +$

$+ \eta_{NO} \cdot \left\{ \left[\dfrac{\left(\frac{S^{p=1}}{\mathcal{R}}\right)}{\ell n\, T} \right]_{NO}^{T_L} \cdot \left(1 - m_{DE}\right) + \left[\dfrac{\left(\frac{S^{p=1}}{\mathcal{R}}\right)}{\ell n\, T} \right]_{NO}^{T_L+100} \cdot m_{DE} \right\}$,

(13) $\sum_i \eta_{i,DE} \cdot \ell n\, \eta_{i,DE} = \eta_{O_2} \cdot \ell n\, \eta_{O_2} + \eta_O \cdot \ell n\, \eta_O + \eta_{N_2} \cdot$

$\ell n\, \eta_{N_2} + \eta_{NO} \cdot \ell n\, \eta_{NO}$,

and

$$(14)\quad p_{DE}^{calc} = p_{\infty}^{\left(\frac{m_{DE}}{m_{air}}\right)} \cdot \frac{T_{DE}^{c_s^{T_{DE}}}}{T_{\infty}^{\left(\frac{m_{DE}}{m_{air}}\right)\cdot c_{s,air}^{T_{\infty}}}} \cdot e^{\left(\frac{m_{DE}}{m_{air}}\right)\cdot\sum_i \eta_{i,\infty}\cdot ln\eta_{i,\infty} - \sum_i \eta_{i,DE}\cdot ln\eta_{i,DE}} .$$

When $p_{DE}^{calc} \neq p_{DE}^{est}$, repeat Steps (2) through (14) with

$$(15)\quad p_{DE}^{est(n+1)} = \xi \cdot p_{DE}^{calc(n)} + (1 - \xi) \cdot p_{DE}^{est(n)} ,$$

where $\xi = 0.5$. Continue the iteration until

$$(16)\quad 100 \cdot \left| \frac{p_{DE}^{calc(n)} - p_{DE}^{est(n)}}{p_{DE}^{calc(n)}} \right| < \Delta p_{DE} = 0.001\% .$$

Then calculate

$$(17)\quad \left(\frac{h_f}{RT}\right)^{T_{DE}} = \eta_{O_2} \cdot \left\{ \left(\frac{H-E_O}{RT}\right)_{O_2}^{T_L} \cdot (1 - m_{DE}) + \left(\frac{H-E_O}{RT}\right)_{O_2}^{T_L+100} \cdot m_{DE} \right\} +$$

$$\eta_O \cdot \left\{ \left(\frac{H-E_O}{RT}\right)_{O}^{T_L} \cdot (1 - m_{DE}) + \left(\frac{H-E_O}{RT}\right)_{O}^{T_L+100} \cdot m_{DE} + \frac{29685}{T_{DE}^{est}} \right\} +$$

$$\eta_{N_2} \cdot \left\{ \left(\frac{H-E_O}{RT}\right)_{N_2}^{T_L} \cdot (1 - m_{DE}) + \left(\frac{H-E_O}{RT}\right)_{N_2}^{T_L+100} \cdot m_{DE} \right\} +$$

$$\eta_{NO} \cdot \left\{ \left(\frac{H-E_O}{RT}\right)_{NO}^{T_L} \cdot (1 - m_{DE}) + \left(\frac{H-E_O}{RT}\right)_{NO}^{T_L+100} \cdot m_{DE} + \frac{10799}{T_{DE}^{est}} \right\}$$

and

$$(18)\quad \underline{\underline{T_{DE}^{calc}}} = \frac{\dot{m}_{DE}}{\dot{m}_{air}} \cdot T_\infty \cdot \frac{\left(\frac{h_f}{RT}\right)_{air}^{T_\infty} + \frac{1}{2}\frac{u_\infty^2 - u_{DE}^2}{R_{air}T_\infty}}{\left(\frac{h_f}{RT}\right)_{DE}^{T_{DE}}} .$$

When $T_{DE}^{calc} \neq T_{DE}^{est}$, repeat steps (1) (see p. 23) through (18) with

$$(19)\quad \underline{\underline{T_{DE}^{est(n+1)}}} = \xi T_{DE}^{calc(n)} + (1 - \xi) \cdot T_{DE}^{est(n)} ,$$

where $\xi = 0.5$. Continue the iterations until

$$(20)\quad 100 \cdot \left| \frac{T_{DE}^{calc(n)} - T_{DE}^{est(n)}}{T_{DE}^{calc(n)}} \right| < \Delta T_{DE} = 0.001\% .$$

The basic configurations of the engine may be pictured as follows:

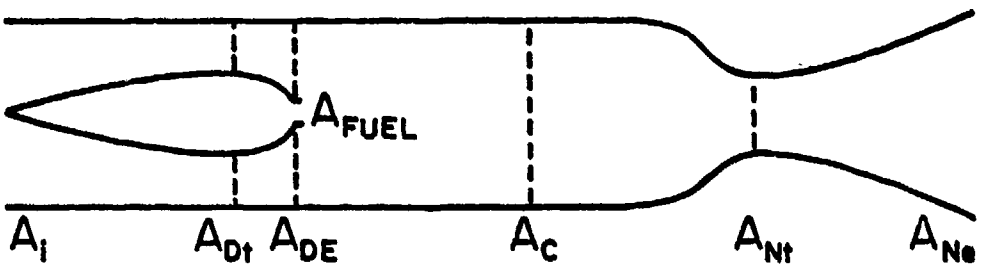

For Subsonic Flow in Combustion Chamber (See Sections 1.a.1 and 2.a.),

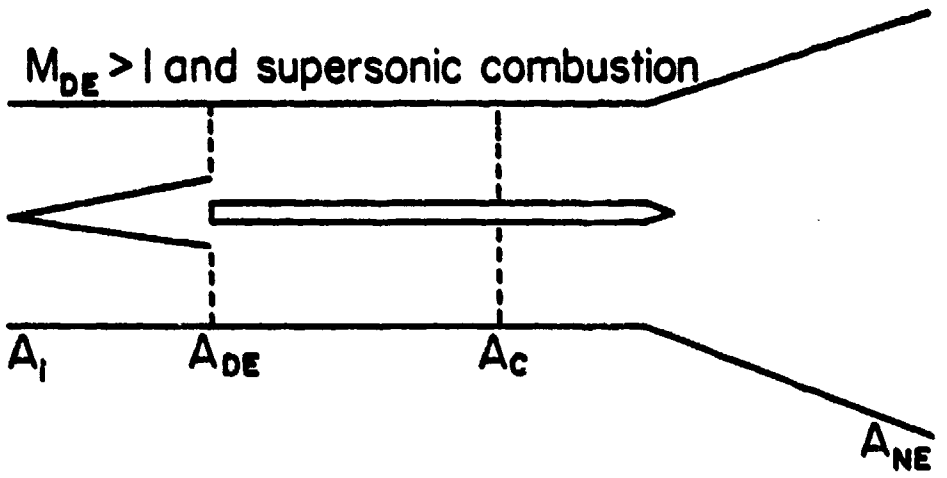

Weak Detonation (See Sections 1.a.2 and 2.b.1)

or

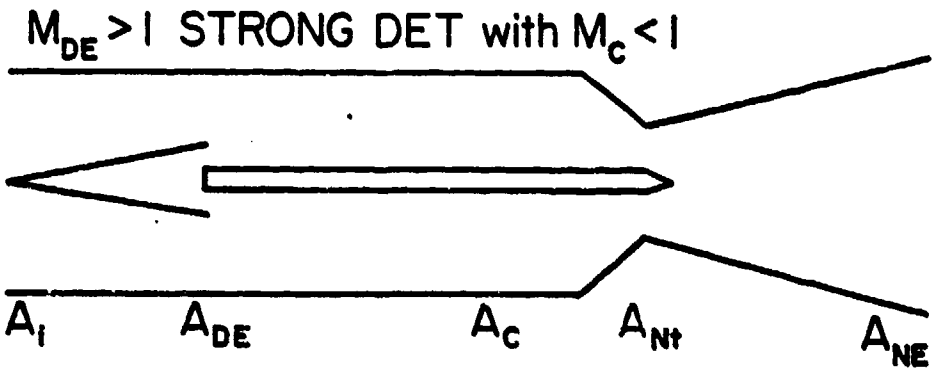

Strong Detonation (Subsonic Combustion Behind N.S.)
with $M_c = 1$ (C.J. Detonation) (See Sections 1.a.2 and 2.b.2)

1.b. Normal Shock Wave at Inlet

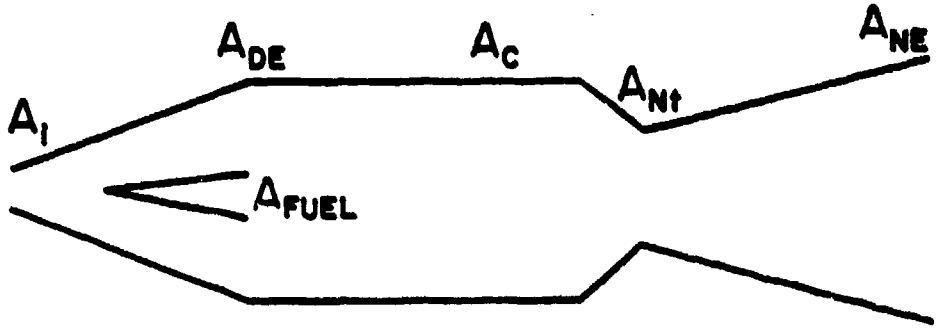

Instead of Eqs. (2) and (3) (see p. 22) use now

$$T_2^{EST} = T_\infty \frac{\left(1 + \frac{\gamma - 1}{2} M_\infty^2\right)\left(\gamma M_\infty^2 - \frac{\gamma - 1}{2}\right)}{\left(\frac{\gamma + 1}{2} M_\infty\right)^2} \qquad (4)$$

and

$$p_2^{EST} = p_\infty \cdot \frac{2\gamma M_\infty^2 - (\gamma - 1)}{\gamma + 1} \qquad (5)$$

} let $\gamma \sim 1.3$ for $M \sim 10$

for the estimates of temperature and pressure behind the normal shock wave attached to the inlet. Then use steps (1) (see p. 23) through (11) to calculate the $\eta_{i,2}$ (steps 1-11 are common to both calculation procedures). Then calculate

$$(12^*)\quad \underline{\underline{\left(\frac{h_f}{RT}\right)^{T_2}}} = \eta_{O_2} \cdot \left(\left(\frac{H-E_o}{\mathcal{R}T}\right)_{O_2}^{T_L} \cdot (1 - m_2) + \left(\frac{H-E_o}{\mathcal{R}T}\right)_{O_2}^{T_L+100} \cdot m_2\right) + m_2$$

$$\eta_O \cdot \left(\left(\frac{H-E_o}{\mathcal{R}T}\right)_{O}^{T_L} \cdot (1 - m_2) + \left(\frac{H-E_o}{\mathcal{R}T}\right)_{O}^{T_L+100} \cdot m_2 + \frac{29685}{T_2^{EST}}\right) +$$

$$\eta_{N_2} \cdot \left(\left(\frac{H-E_o}{\mathcal{R}T}\right)_{N_2}^{T_L} \cdot (1 - m_2) + \left(\frac{H-E_o}{\mathcal{R}T}\right)_{N_2}^{T_L+100} \cdot m_2\right) +$$

$$\eta_{NO} \cdot \left(\left(\frac{H-E_o}{\mathcal{R}T}\right)_{NO}^{T_L} \cdot (1 - m_2) + \left(\frac{H-E_o}{\mathcal{R}T}\right)_{NO}^{T_L+100} \cdot m_2 + \frac{10799}{T_2^{EST}}\right).$$

This calculation of $\frac{h_f}{RT}$ is identical to that of step (17) of the previous procedure with the exception that T_{DE} has been replaced by T_2. Then calculate

$$(13^*)\quad \underline{\underline{p_2^{calc}}} = p_\infty \cdot \left[B + \sqrt{B^2 + \frac{T_2^{EST}}{T_\infty} \cdot \frac{m_{air}}{m_2}} \right],$$

where

$$B = \frac{T_2^{EST}}{T_\infty} \cdot \frac{m_{air}}{m} \left(\frac{h_f}{RT}\right)_{DA}^{T_2^{EST}} - \left(\frac{h_f}{RT}\right)_{air}^{T_\infty} - \frac{1}{2}\left(\frac{T_2^{EST}}{T_\infty} \cdot \frac{m_{air}}{m_2} - 1\right).$$

When $p_2^{calc} \neq p_2^{est}$, repeat steps (1) through (11), (12*), and (13*) with

$$(14^*)\quad \underline{\underline{p_2^{est(n+1)}}} = \xi p_2^{calc(n)} + (1 - \xi)\, p_2^{est(n)},$$

where $\xi = 0.5$. Continue the iteration until

$$(15^*)\quad 100 \cdot \left| \frac{p_2^{calc(n)} - p_2^{est(n)}}{p_2^{calc(n)}} \right| < \Delta p_2 = 0.001\%.$$

Then calculate

$$(16^*)\quad \underline{\underline{T_2^{calc}}} = T_\infty \cdot \left[\frac{m_2}{m_{air}} \frac{\left(\frac{h_f}{RT}\right)_{air}^{T_\infty} + 0.7M_\infty^2 \left(1 - \left[\frac{T_2^{EST}}{T_\infty} \cdot \frac{m_{air}}{m_2} \cdot \frac{p_\infty}{p_2}\right]^2\right)}{\left(\frac{h_f}{RT}\right)_{DA}^{T_2^{EST}}} \right].$$

When $T_2^{calc} \neq T_2^{est}$, repeat steps (1) through (11) and (12*) through (16*)

$$(17^*)\quad \underline{\underline{T_2^{est(n+1)}}} = \xi \cdot T_2^{calc} + (1 - \xi)\, T_2^{est},$$

where ξ is as before. Continue the iteration until

$$(18^*)\quad 100 \cdot \left| \frac{T_2^{calc(n)} - T_2^{est(n)}}{T_2^{calc(n)}} \right| < \Delta T_2 = 0.001\%.$$

Then calculate

$$(9^*) \quad u_2 = u_\infty \cdot \frac{T_2}{T_\infty} \cdot \frac{p_\infty}{p_2} \cdot \frac{m_{air}}{m_2} .$$

If u_2 is larger than practical, subsonic diffusion from u_2 to u_{DE} is necessary. These calculations are identical with those given in Section 1.a. when the subscript ∞ is replaced by the subscript 2.

1.c. One Oblique Shock Wave Followed by a Normal Shock Wave

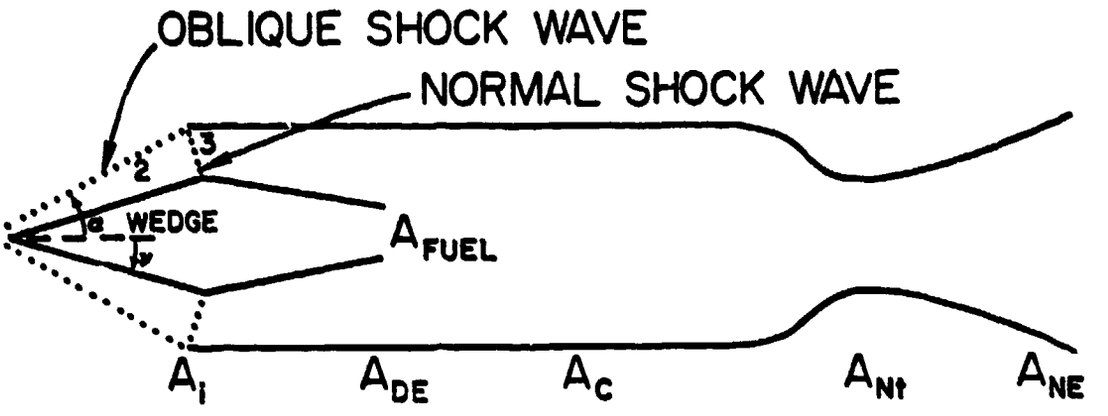

Use the equations of Section 1.b. but replace u_∞ by $u_{\infty,u} = u_\infty \cdot \sin\sigma$, where σ is the angle of the shock wave formed by the wedge (see sketch above; σ is given!). Replace M_∞ by $M_{\infty,n} = M_\infty \cdot \sin\sigma$. With the values of $u_{\infty,n}(M_{\infty,n})$, T_a, and p_a calculate the state of the air behind the oblique shock by the procedure outlined in Section 1.b. These calculations lead to p_2, T_2, and $u_{2,n}$. The gas speed parallel to the wedge is

$$u_2 = \sqrt{u_{2,n}^2 + (u_\infty \cdot \cos\sigma)^2} \qquad (M_2 > 1)$$

and the half angle of the wedge is

$$\delta = \sigma - \tan^{-1}\left(\frac{u_{2,n}}{u_\infty \cdot \cos\sigma}\right).$$

Then calculate the conditions behind the normal shock wave which are designated by the subscript 3. For the first estimate of T_3 and p_3 use instead of Eqs. (4 and 5):

$$T_3^{EST} = T_2 \frac{\left(1 + \frac{\gamma - 1}{2\gamma}\frac{u_2^2}{\mathcal{R}T_2} \cdot m_2\right) \cdot \left(\frac{u_2^2 m_2}{\mathcal{R}T_2} - \frac{\gamma - 1}{2}\right)}{\left(\frac{\gamma + 1}{2}\right)^2 \cdot \frac{u_2^2}{\gamma\mathcal{R}T_2} \cdot m_2} \qquad (6)$$

and

$$p_3^{EST} = p_2 \cdot \left[\frac{2}{\gamma + 1} \cdot \frac{u_2^2}{\mathcal{R}T_2} \cdot m_2 - \frac{\gamma - 1}{\gamma + 1}\right]. \qquad (7)$$

use $\gamma = 1.3$

If $u_3 > u_{DE}$, it is necessary to employ subsonic diffusion from u_3 to u_{DE} by means of the calculations developed in Section 1.a. The subscript ∞ is replaced by the subscript 3. In step (16*) the term $0.7M_\infty^2$ is replaced by $\frac{u_2^2}{2\mathcal{R}T_2} \cdot m_2$.

2. Calculation of State of Combustion Gas

From continuity and momentum equations

$$T_c = \frac{u_c}{\left(\frac{\mathcal{R}}{m_c}\right)}\left[u_{c,max}^{(M-C)} - u_c\right], \qquad (8)$$

where

$$u_{c,max}^{(M-C)} = \left\{\frac{f \cdot u_{FUEL}\left[1 + \frac{p_{FUEL}}{\rho_{FUEL}u_{FUEL}^2}\right] + u_{DE}\left[1 + \frac{\mathcal{R}T_{DE}}{m_{DE}u_{DE}^2}\right]}{1 + f}\right\}.$$

From the energy equation we obtain

$$u_c = \sqrt{\left(u_{c,max}^{(E)}\right)^2 - 2\frac{\mathcal{R}T_c}{m_c}\left(\frac{h_f}{RT}\right)_c^{T_c}}, \qquad (9)$$

where

$$\left(u_{c,max}^{(E)}\right)^2 = \frac{f\left[h_{f,FUEL}^{T_{FUEL}} + \frac{u_{FUEL}^2}{2}\right] + h_{fDA}^{T_{DE}} + \frac{u_{DE}^2}{2}}{\frac{1}{2}(1+f)} .$$

Substitution of Eq. (8) into Eq. (9) leads to

$$u_c = u_{c,max}^{(M-C)} \cdot \frac{\Sigma}{2\Sigma - 1}\left[1 \pm \sqrt{1 - \left(\frac{u_{c,max}^{(E)}}{u_{c,max}^{(M-C)}}\right)^2 \cdot \frac{2\Sigma - 1}{\Sigma^2}}\right], \qquad (10)$$

where

$$\Sigma = \left(\frac{H_f}{RT}\right)_c^{T_c} = \sum \eta_{i,c}\left(\frac{H_f}{\Re T}\right)_i^{T_c} .$$

Since $\eta_{i,c}$ depend on T_c and p_c, the calculation of the state of the combustion gas (T_c, u_c, p_c) consists of an iterative procedure comprising three loops. The inner loop consists of the calculation of the $\eta_{i,c}$. Use $T_c^{EST} \sim T_{DE} + 1500$ K and

$$p_c^{EST} \approx p_{DE} ;$$

$$\frac{T_c^{EST} - T_L}{100} = m_c .$$

$$\underline{\underline{K^{(0)}}} = \left[a^{(0)}(T_L)\right]^{(1-m_c)} \cdot \left[a^{(0)}(T_L + 100)\right]^{m_c} \cdot \sqrt{T_c^{EST}} \cdot e^{-\frac{29685}{T_c^{EST}}} \cdot \frac{1}{\sqrt{p_c^{EST}}} ;$$

$$\underline{\underline{K^{(H_2O)}}} = \left[a^{(H_2O)}(T_L)\right]^{(1-m_c)} \cdot \left[a^{(H_2O)}(T_L + 100)\right]^{m_c} \cdot \frac{1}{\sqrt{T_c^{EST}}} e^{\frac{28736}{T_c^{EST}}} \cdot \sqrt{p_c^{EST}} ;$$

$$\underline{\underline{K^{(OH)}}} = \left[a^{(OH)}(T_L)\right]^{(1-m_c)} \cdot \left[a^{(OH)}(T_L + 100)\right]^{m_c} e^{-\frac{4675}{T_c^{EST}}};$$

$$\underline{\underline{K^{(H)}}} = \left[a^{(H)}(T_L)\right]^{(1-m_c)} \cdot \left[a^{(H)}(T_L + 100)\right]^{m_c} \cdot \sqrt{T_c^{EST}} \; e^{-\frac{25982}{T_c^{EST}}} \cdot \frac{1}{\sqrt{p_c^{EST}}};$$

$$\underline{\underline{K^{(CO_2)}}} = \left[a^{(CO_2)}(T_L)\right]^{(1-m_c)} \cdot \left[a^{(CO_2)}(T_L + 100)\right]^{m_c} \cdot \left(T_c^{EST}\right)^{0.125} \cdot e^{\frac{33598}{T_c^{EST}}} \cdot \sqrt{p_c^{EST}};$$

$$\underline{\underline{K^{(NO)}}} = \left[a^{(NO)}(T_L)\right]^{(1-m_c)} \cdot \left[a^{(NO)}(T_L + 100)\right]^{m_c} \cdot e^{-\frac{10799}{T_c^{EST}}} \cdot$$

Use $\eta_{O_2}^{EST} = 0.01$; then calculate

$$\underline{\underline{\eta_O}} = K^{(O)} \cdot \sqrt{\eta_{O_2}^{EST}} \cdot$$

$$A = 0.25\left[\left(\frac{\nu_{O_2}^g + \nu_{N_2}^g}{\nu_{H_2}^g} + 1 + \frac{\nu_c^g}{2\nu_{H_2}^g} \cdot \frac{1}{K^{CO_2}\sqrt{\eta_{O_2}} + 1}\right)\left(K^{OH} \cdot \sqrt{\eta_{O_2}} + K^H\right) + K^H\right];$$

$$B = \left(\frac{\nu_{O_2}^g + \nu_{N_2}^g}{\nu_{H_2}^g} + 0.5 + \frac{\nu_c^g}{2\nu_{H_2}^g} \cdot \frac{1}{K^{CO_2}\sqrt{\eta_{O_2}} + 1}\right)\left(K^{H_2O} \cdot \sqrt{\eta_{O_2}} + 1\right) + 0.5 \cdot$$

$$\eta_{H_2} = \left\{\sqrt{\left(\frac{A}{B}\right)^2 + \frac{1 - 0.5\eta_O}{B}} - \frac{A}{B}\right\}^2,$$

$$\eta_{H_2O} = K^{(H_2O)} \cdot \sqrt{\eta_{O_2}} \cdot \eta_{H_2},$$

$$\eta_{OH} = K^{(OH)} \cdot \sqrt{\eta_{O_2}} \cdot \sqrt{\eta_{H_2}} ,$$

$$\eta_{H} = K^{(H)} \cdot \sqrt{\eta_{H_2}} ,$$

$$\eta_{CO} = \frac{\nu_c^g}{\nu_{H_2}^g} \cdot \frac{\eta_{H_2O} + \eta_{H_2} + \frac{1}{2}\left(\eta_{OH} + \eta_{H}\right)}{1 + K^{(CO_2)} \cdot \sqrt{\eta_{O_2}}} ,$$

$$\eta_{CO_2} = K^{(CO_2)} \cdot \eta_{CO} \cdot \sqrt{\eta_{O_2}} ,$$

$$\eta_{N_2} = \left\{ \sqrt{\left[\frac{1}{4} K^{(NO)} \cdot \sqrt{\eta_{O_2}}\right]^2 + \frac{\nu_{N_2}^g}{\nu_{H_2}^g}\left(\eta_{H_2O} + \eta_{H_2} + \frac{1}{2}\left(\eta_{OH} + \eta_{H}\right)\right)} \right.$$

$$\left. - \frac{1}{4} K^{(NO)} \cdot \sqrt{\eta_{O_2}} \right. ,$$

$$\eta_{NO} = K^{(NO)} \cdot \sqrt{\eta_{N_2}} \cdot \sqrt{\eta_{O_2}} , \text{ and}$$

$$\eta_{O_2}^{calc} = \frac{\nu_{O_2}^g}{\nu_{H_2}^g}\left(\eta_{H_2O} + \eta_{H_2} + \frac{1}{2}\eta_{OH} + \frac{1}{2}\eta_{H}\right) - \eta_{CO_2}$$

$$- \frac{1}{2}\left(\eta_{CO} + \eta_{H_2O} + \eta_{OH} + \eta_{O} + \eta_{NO}\right) .$$

when $\eta_{O_2}^{calc} \neq \eta_{O_2}^{est}$ repeat calculations

with

$$\eta_{O_2}^{EST(n+1)} = \xi \eta_{O_2}^{calc(n)} + (1 - \xi)\, \eta_{O_2}^{est(n)}$$

until

$$100 \left| \frac{\eta_{O_2}^{calc(n)} - \eta_{O_2}^{est(n)}}{\eta_{O_2}^{calc(n)}} \right| < \Delta\eta_{O_2} = 0.00001\% .$$

In the second loop the p_c is calculated so that it is compatible with the estimated temperature T_c^{EST}. From the continuity equation and with the condition that

$$A_c = A_{DE} + A_{FUEL}$$

we obtain

$$p_c^{calc} = \frac{T_c}{m_c \cdot u_c} \cdot \frac{1 + f}{\frac{f}{\mathcal{R}\rho_{FUEL} u_{FUEL}} + \frac{T_{DE}}{m_{DE} u_{DE} p_{DE}}} .$$

When $p_c^{calc} \neq p_c^{est}$ all previous calculations $(\eta_{i,c})$ are repeated with

$$p_c^{est(n)} = \xi \cdot p_c^{calc(n-1)} + (1 - \xi)\, p_c^{est(n-1)}$$

until

$$100 \left| \frac{p_c^{calc(n)} - p_c^{est(n)}}{p_c^{calc(n)}} \right| < \Delta p_c = 0.0001\% .$$

Now we calculate the formation enthalpy of the combustion gas;

$$\left(\frac{h_f}{RT}\right)_c^{T_c} = \eta_{O_2} \left(\left(\frac{H-E_o}{\mathcal{R}T}\right)_{O_2}^{T_L} (1 - m_c) + \left(\frac{H-E_o}{\mathcal{R}T}\right)_{O_2}^{T_L+100} \cdot m_c \right) +$$

$$\eta_{H_2} \left(\left(\frac{H-E_o}{\mathcal{R}T}\right)_{H_2}^{T_L} (1 - m_c) + \left(\frac{H-E_o}{\mathcal{R}T}\right)_{H_2}^{T_L+100} \cdot m_c \right) +$$

$$\eta_{N_2} \left(\left(\frac{H-E_o}{\mathcal{R}T}\right)_{N_2}^{T_L} (1 - m_c) + \left(\frac{H-E_o}{\mathcal{R}T}\right)_{N_2}^{T_L+100} \cdot m_c \right) +$$

$$\eta_{CO_2} \left(\left(\frac{H-E_o}{\mathcal{R}T}\right)_{CO_2}^{T_L} (1 - m_c) + \left(\frac{H-E_o}{\mathcal{R}T}\right)_{CO_2}^{T_L+100} \cdot m_c - \frac{47286}{T_c^{EST}} \right) +$$

$$\eta_{CO} \left(\left(\frac{H-E_o}{\mathcal{R}T}\right)_{CO}^{T_L} (1 - m_c) + \left(\frac{H-E_o}{\mathcal{R}T}\right)_{CO}^{T_L+100} \cdot m_c - \frac{13688}{T_c^{EST}} \right) +$$

$$\eta_{H_2O} \left(\left(\frac{H-E_o}{\mathcal{R}T}\right)_{H_2O}^{T_L} (1 - m_c) + \left(\frac{H-E_o}{\mathcal{R}T}\right)_{H_2O}^{T_L+100} \cdot m_c - \frac{28736}{T_c^{EST}} \right) +$$

$$\eta_{OH}\left(\left(\frac{H-E_o}{\Re T}\right)_{OH}^{T_L}(1-m_c)+\left(\frac{H-E_o}{\Re T}\right)_{OH}^{T_L+100}\cdot m_c+\frac{4675}{T_c^{EST}}\right)+$$

$$\eta_{O}\left(\left(\frac{H-E_o}{\Re T}\right)_{O}^{T_L}(1-m_c)+\left(\frac{H-E_o}{\Re T}\right)_{O}^{T_L+100}\cdot m_c+\frac{29685}{T_c^{EST}}\right)+$$

$$\eta_{H}\left(\left(\frac{H-E_o}{\Re T}\right)_{H}^{T_L}(1-m_c)+\left(\frac{H-E_o}{\Re T}\right)_{H}^{T_L+100}\cdot m_c+\frac{25982}{T_c^{EST}}\right)+$$

$$\eta_{NO}\left(\left(\frac{H-E_o}{\Re T}\right)_{NO}^{T_L}(1-m_c)+\left(\frac{H-E_o}{\Re T}\right)_{NO}^{T_L+100}\cdot m_c+\frac{10799}{T_c^{EST}}\right),$$

and then u_c according to Eq. (10) and T_c according to Eq. (8). When $T_c^{calc} \neq T_c^{est}$ all iterations ($\eta_{i,c}$ and p_c) have to be repeated with

$$T_c^{EST(n)} = \xi T_c^{calc(n-1)} + (1-\xi)^{est(n-1)},$$

when $$u_c^{calc} < \frac{1}{2} u_{c,max}^{(M-C)},$$

and

$$T_c^{EST(n)} = (1+\xi)\, T_c^{EST(n-1)} - \xi T_c^{calc(n-1)},$$

when $$u_c^{calc} > \frac{1}{2} u_{c,max}^{(M-C)}$$

3. Calculation of Exhaust Speed, u_e, Specific Thrust, and Thrust Specific Fuel Consumption

a. The Expansion is Assumed to be Isentropic and Complete So That $p_e = p_a$

With an estimate of the temperature at the nozzle exit from the simplified entropy equation the $\eta_{i,e}$ are calculated by the same scheme as used for the $\eta_{i,c}$ calculation. Then the nozzle exit temperature is calculated from the entropy equation

$$T_e^{calc} = T_c^{\left(\frac{c_s^{T_c}}{c_s^{T_e}} \cdot \frac{m_e}{m_c}\right)} \left[\frac{p_e}{p_c\left(\frac{m_e}{m_c}\right)}\right]^{\frac{1}{c_s^{T_e}}} \cdot e^{\frac{\sum \eta_{i,e} \ln \eta_{i,e} - \frac{m_e}{m_c} \sum \eta_{i,c} \ln \eta_{i,c}}{c_s^{T_e}}},$$

where

$$c_s^{T_e} = \sum \eta_{i,e} \left[\frac{\left(\frac{S^{p=1}}{\mathcal{R}}\right)}{\ln T}\right]_i^{T_e} .$$

When $T_e^{calc} \neq T_e^{est}$, the calculations are repeated with new estimates of T_e obtained from the equation

$$T_e^{est(n)} = \xi T_e^{calc(n-1)} + (1 - \xi)\, T_e^{est(n-1)}$$

until $$100 \cdot \left|\frac{T_e^{calc(n)} - T_e^{est(n)}}{T_e^{calc(n)}}\right| < 0.001\% .$$

The speed of the exhaust jet is then

$$u_e = \sqrt{u_c^2 + 2h_{f,c}^{T_e} - 2h_{f,e}^{T_e}}$$

or

$$u_e = \sqrt{u_c^2 + 2\left[\frac{\mathcal{R}T_c}{m_c}\left(\frac{h_f}{RT}\right)_c^{T_c} - \frac{\mathcal{R}T_e}{m_e}\left(\frac{h_f}{RT}\right)_e^{T_e}\right]} .$$

The specific thrust is

$$F_s = (1 + f)\, u_e - u_F$$

and the thrust specific fuel consumption is

$$F_{sfc} = \frac{3600\, f}{F_s} \left[\frac{kg/h}{N}\right] .$$

b. The Expansion is Incomplete (Convergent Nozzle with $M_e = 1$)

For an estimated value of the exit temperature $\left(T_e = T_e^{EST} = 0.87\ T_c\right)$ together with an estimate of the pressure at the nozzle exit, $p_e = p_e^{EST} = 0.53\ p_c$, the $\eta_{i,e}$ are calculated first. Then the entropy equation is used to determine the pressure which is compatible with the estimated temperature

$$p_e^{calc} = p_c \cdot \frac{\frac{\dot{m}_e}{\dot{m}_c}}{\left(\frac{\dot{m}_e}{\dot{m}_c}\right) \cdot c_s^{T_c}} \cdot \frac{T_e^{c_s^{T_e}}}{T_c} \cdot e^{\frac{\dot{m}_e}{\dot{m}_c} \sum \eta_{i,c} \ln \eta_{i,c} - \sum \eta_{i,e} \ln \eta_{i,e}} .$$

When $p_e^{calc} \neq p_e^{est}$ the iteration is continued with

$$p_e^{est(n)} = \xi p_e^{calc(n-1)} + (1 - \xi)\ p_e^{est(n-1)}$$

until

$$100 \left| \frac{p_e^{calc(n)} - p_e^{est(n)}}{p_e^{calc(n)}} \right| < \Delta p_e = 0.001\% .$$

(Note: for each new p_e^{est} a new set of $\eta_{i,e}$ must be calculated.)

Now with the energy equation

$$u_e^2 = u_c^2 + 2\left[h_{f,c}^{T_c} - h_{f,e}^{T_e}\right]$$

and the condition that $u_e^2 = w_{a,e}^2 = \gamma_e^{T_e} \frac{\mathcal{R} T_e}{\dot{m}_e}$,

a calculated exit temperature, T_e^{calc}, is determined from the following form of the energy equation:

$$\gamma_e^{T_e} \cdot \frac{\mathcal{R}}{\dot{m}_e} T_e = u_c^2 + 2\left[\frac{\mathcal{R} T_c}{\dot{m}_c}\left(\frac{h_f}{RT}\right)_c^{T_c} - \frac{\mathcal{R} T_e}{\dot{m}_e}\left(\frac{h_f}{RT}\right)_e^{T_e}\right]$$

which leads to

$$T_e^{calc} = \frac{u_c^2 + 2\,\frac{\mathcal{R}T_c}{m_c}\left(\frac{h_f}{RT}\right)_c^{T_c}}{\frac{\mathcal{R}}{m_e}\left[\gamma_e^{T_e} + 2\left(\frac{h_f}{RT}\right)_e^{T_e^{EST}}\right]} .$$

When $T_e^{calc} \neq T_e^{est}$, all three iterations $(\eta_{i,e}, p_e, \text{and } T_e)$ are repeated with

$$T_e^{est(n)} = \xi T_e^{calc(n-1)} + (1 - \xi)\, T_e^{est(n-1)}$$

until

$$100 \left| \frac{T_e^{calc(n)} - T_e^{est(n)}}{T_e^{calc(n)}} \right| < \Delta T_e = 0.001\% .$$

Then the exhaust speed is calculated

$$u_e = \sqrt{u_c^2 + 2\left[\frac{\mathcal{R}T_c}{m_c}\left(\frac{h_f}{RT}\right)_c^{T_c} - \frac{\mathcal{R}T_e}{m_e}\left(\frac{h_f}{RT}\right)_e^{T_e}\right]},$$

$$F_s = (1 + f)\, u_e - u_F + (1 + f)\, u_e \left[\frac{\mathcal{R}T_e}{m_e u_e^2}\left(1 - \frac{p_a}{p_e}\right)\right], \text{ or}$$

$$F_s = (1 + f)\, u_{e,eff} - u_F ,$$

where

$$u_{e,eff} = u_e \left[1 + \frac{\mathcal{R}T_e}{m_e u_e^2}\left(1 - \frac{p_a}{p_e}\right)\right]$$

and

$$F_{sfc} = \frac{3600\, f}{F_s}\left[\frac{kg/h}{N}\right] .$$

4. The Cross-Sectional Area, A_x, at Station x Along the Ramjet Engine According to the Continuity Equation Is

$$\frac{A_x}{A_i} = \frac{u_i \mathfrak{m}_i p_i}{T_i \cdot p_x} \sqrt{\frac{T_x}{\gamma_x^{T_x} \mathfrak{R} \mathfrak{m}_x}} .$$

For operation at design conditions $u_i = u_\infty$, $\mathfrak{m}_i = \mathfrak{m}_{air}$, $p_i = p_\infty$, and $T_i = T_\infty$. For $x = Dt$ (diffuser throat) the procedure described in the previous section for the short nozzle must be used. For estimated values of T_{Dt} and p_{Dt}

$$T_{Dt} \simeq \frac{T_\infty \left(1 + \frac{\gamma - 1}{2} M_\infty^2\right)}{\frac{\gamma + 1}{2}}$$

and

$$p_{Dt} = p_\infty \cdot \left(\frac{T_{Dt}}{T_\infty}\right)^{\frac{\gamma}{\gamma - 1}}$$

the η_i of the dissociated air are calculated as given in the first section. Then the pressure p_{Dt} which is compatible with the estimated temperature is obtained by iteration

$$p_{Dt}^{calc} = p_\infty^{\frac{\mathfrak{m}_{Dt}}{\mathfrak{m}_{air}}} \cdot \frac{T_{Dt}^{c_s^{T_{Dt}}}}{\frac{\mathfrak{m}_{Dt}}{\mathfrak{m}_{air}} \cdot c_s^{T_\infty}} \cdot e^{\frac{\mathfrak{m}_{Dt}}{\mathfrak{m}_{air}} \sum \eta_{i\infty} \ln \eta_{i\infty} - \sum \eta_{i,Dt} \ln \eta_{i,Dt}}$$

T_∞

and

$$T_{Dt}^{calc} = \frac{u_\infty^2 + 2 \frac{\mathfrak{R} T_\infty}{\mathfrak{m}_{air}} \left(\frac{h_f}{RT}\right)_{air}^{T_\infty}}{\frac{\mathfrak{R}}{\mathfrak{m}_{Dt}} \left[\gamma_{Dt}^{T_{Dt}} + 2 \left(\frac{h_f}{RT}\right)_{Dt}^{T_{Dt}}\right]} .$$

REFERENCES

1. Edse, R., and Lawrence, Jr., L. R., Detonation Induction Phenomena and Flame Propagation Rates in Low Temperature Hydrogen-Oxygen Mixtures, Combustion and Flame Journal, V. 13, 479-486 (October, 1969).

2. Bollinger, L. E., Fong, M. C., and Edse, R., Detonation Induction Distances in Combustible Gaseous Mixtures at Atmospheric and Elevated Initial Pressures, WADC Technical Report 58-591 (August, 1959).

3. Edse, R., Ignition, Combustion, Detonation, and Quenching of Reactive Mixtures, AFOSR-TR, (November, 1975).